Annals of Nuclear Energy 176 (2022) 109243

Contents lists available at ScienceDirect

Annals of Nuclear Energy

journal homepage: www.elsevier.com/locate/anucene

Mechanical model for the motion of RPV internals affecting neutron flux noise

Christoph Bläsius [a,*], Joachim Herb [b], Jürgen Sievers [a], Alexander Knospe [c], Marco Viebach [c], Carsten Lange [c]

[a] Gesellschaft für Anlagen- und Reaktorsicherheit gGmbH, Schwertnergasse 1, 50667 Cologne
[b] Gesellschaft für Anlagen- und Reaktorsicherheit gGmbH, Boltzmannstraße 14, 85748 Garching
[c] Technische Universität Dresden, Institut für Energietechnik, George-Bähr-Straße 3b, 01069 Dresden

ARTICLE INFO

Article history:
Received 22 February 2022
Received in revised form 20 May 2022
Accepted 25 May 2022
Available online 25 June 2022

Keywords:
RPV internals
Neutron flux noise
Flow-induced vibration
Fluid–structure interaction
Reduced order model

ABSTRACT

In the decade after 2000, the amplitude of the neutron flux fluctuations in German 1300 MW_e class PWR built by Kraftwerk Union (KWU) increased and later decreased significantly. To further investigate the hypothesis that changes in the mechanical properties of the fuel assemblies (FAs) and subsequent stronger mechanical oscillations of fuel assemblies and other RPV internals are responsible for the observations and to find possible excitation mechanisms, a simple mechanical model is developed. It describes the dynamic motion response of the mechanically coupled system of Reactor Pressure Vessel (RPV), core barrel and a row of fuel assemblies and takes reactive fluidic forces into account. To determine the components to be considered in this model, RPV internals with an effect on neutron flux are identified in a prior step.

The dynamic answers of the model to generic excitation scenarios and parametric studies reveal distinct properties of the system. They indicate 1) that fluidic near-field coupling can equalize the fuel assemblies' reaction amplitudes within a certain region regardless of their individual stiffnesses, 2) that the fluid must be part of the oscillation, 3) that a non-periodicity might stem from a superposition and interaction of several oscillators, 4) that a local excitation source does not spread or synchronize over the whole core, 5) that a neglection or separate consideration of the RPV and core barrel may be justified in some cases. The findings altogether affirm that core-wide oscillations of the fluid flow leading to a simultaneous oscillation of individual fuel assembly groups, possibly including bidirectional effects between fluid and structure, in combination with the changes of the fuel assemblies' mechanical properties, might be responsible for the temporary increase of neutron flux fluctuations observed in PWR built by KWU.

A variant of the mechanical model was studied in a full core investigation with coupled neutron kinetics simulations. These simulations qualitatively reproduce important features of measurement data, while being overall too small in amplitude to explain the observations quantitatively, which confirmed the necessity of considering further effects.

1. Introduction

In the decade after 2000, the amplitude of the neutron flux fluctuations in German 1300 MW_e class PWR built by Kraftwerk Union (KWU) increased and later decreased significantly (Seidl et al., 2015). This is one of the reasons why the EU Horizon 2020 project CORTEX (Demazière et al., 2018) was initiated to analyze neutron flux fluctuations in more detail. One of the hypotheses to explain these changes are different mechanical properties of the fuel assemblies (FAs) used during this period. These changes might have resulted in a stronger mechanical response of the fuel assemblies and other mechanically coupled internals of the Reactor Pressure Vessel (RPV) to the forces of the coolant flow, which consequently influenced the neutron flux (Herb et al., 2018).

The characteristics of the signal component that increased during the aforementioned period has been known for a long time and is specific for reactors built by KWU (Grondey et al., 1991; Fiedler, 2002), but a clear attribution to an underlying phenomenon has never been successful. It is characterized by an opposite behavior of the core halves, an in-phase behavior over the core height and a $1/\omega^2$-shaped course with peak at about 0.8–1 Hz (Herb et al., 2018; Pohlus and Paquée, 2018). In the past, it was often attributed to thermal hydraulic effects especially due to its low frequency and

* Corresponding author.

https://doi.org/10.1016/j.anucene.2022.109243
0306-4549/

frequency spectrum shape (Fry et al., 1984), but the recent findings and subsequent signal analysis campaigns have given reason to take mechanical motions of RPV internals into account as part of the explanation and take further steps to identify the underlying physics of this phenomenon in detail.

Therefore, four main parts of work have been conducted, which are described in this paper. First, mechanical components with an effect on neutron flux during oscillation and corresponding excitation mechanisms are identified by conducting a literature study. These include well known, but also hypothetic and only defect-related phenomena. In a next step, based on the original idea of (Bauernfeind, 1977), a simple mechanical model of the RPV, core barrel and a row of fuel assemblies, implemented in the structure mechanical code ANSYS Mechanical (ANSYS Inc., 2019), is generated. The model takes into account the mechanical coupling between the components and reactive forces of the fluid via an added mass/stiffness/damping approach. It is fed with generic excitation scenarios to learn more about the dynamic behavior of the system. Parametric studies are conducted to investigate the influence of core loading pattern, damping and near-field coupling. In a last step, a variant of the mechanical model is coupled to the reactor dynamics code DYN3D to perform full core investigations of the influence of mechanical vibrations of core components on the neutron flux signals.

2. Mechanical oscillations with effect on neutron flux signals

2.1. Detection of mechanical oscillations in neutron flux signals

Current western PWR are equipped with detectors for the measurement of neutron flux in the operational power range inside and outside the reactor core. Their original purpose is the monitoring of the reactor power and power density distribution in the core. Nevertheless, investigations showed very early that the signals noise components contain additional valuable information about further conditions inside the core, where it is impossible or impractical to install diagnostic instrumentation due to limited space, temperature and radiation (Fry et al., 1984). Apart from the inherent noise from the stochastic nature of the chain reaction, noise due to temperature and density variations of the moderator (e.g. subcooled boiling, temperature plumes, transport effects, turbulence, pressure pulsations), modulations of the neutron flux by mechanical oscillations (geometry noise), and noise from the detector and signal processing chain can be found in the noise signal. Neutron noise analysis was subsequently used for various purposes, such as research on neutron kinetic stability problems (Sunder, 1985), determination of reactivity coefficients, monitoring of thermal hydraulic conditions (Runkel, 1987) as well as monitoring of mechanical properties of core internals and primary circuit components for damage detection (Fry et al., 1984). The latter has become an important part of damage monitoring concepts of today's power reactors. For some components, there even is no further measurement available for the online monitoring of mechanical integrity (Sunder, 1985).

Apart from particularly prominent peaks in the auto power spectral density (APSD) chart of the neutron flux measurement, the correct assignment of signals to mechanical oscillation modes can be difficult, hypothetical, or ambiguous, as they can be weak or visible only in case of a defect (Fig. 1). Furthermore, apart from isolated individual vibrations, coupled oscillators with partly chaotic characteristics (e.g. double pendulum configurations or collisions) and broadband effects on neutron flux noise can be found within the system. Therefore, the correct assignment is often supported by correlations between different neutron flux sensors or correlations with other sensor types, as vibration sensors mounted outside the RPV, structure-borne sound measurements or pressure transducers of the primary circuit (Thie, 1981). Mechanical models of the RPV internals (see section 3.1) and heavily instrumented mock-up experiments, such as the SAFRAN test loop (Damiano and Kryter, 1990; Au-Yang et al., 1995) have been used in the past as well. Several authors have proposed assignments of neutron flux, vibration measurement and pressure transducer signals to mechanical oscillation modes of RPV internals and other effects, such as (Runkel, 1987) for KWU 1300 MW_e class PWR or (Thie, 1981; Fry et al., 1984; Sunder, 1985; Bauernfeind, 1988; Wach and Sunder, 1989; Stegemann and Runkel, 1995; Fiedler, 2002). In the following, an overview over the oscillating components and excitation mechanisms described in literature is given.

2.2. Oscillating components

2.2.1. Fuel assemblies

While in subsection 2.2, oscillating RPV internals with effect on neutron flux are discussed, the corresponding excitation mechanisms are discussed separately in subsection 2.3. Certainly, the most important oscillators with effect on neutron flux are the fuel assemblies. Regarding oscillation modes, fuel assemblies can be either idealized as cantilevered beam, simply supported beam or simply supported beam with complete fixation at one end (Fig. 2). The real oscillation mode is much more complex, nonlinear and cannot be entirely described mathematically due to the complex bearing characteristics and the inhomogeneous stiffness distribution. This also leads to a dependency of lateral stiffness and natural frequency from the oscillation amplitude (Sunder, 1985). Realistic deflection shapes of fuel assemblies for large amplitudes have been measured and simulated in (Jeon et al., 2009; Ricciardi, 2016; Wanninger et al., 2016b). Due to their slenderness, fuel assemblies show the lowest natural frequencies among the RPV internals. For KWU 1300 MW_e class PWR, values as low as 0.8 Hz (cantilevered beam mode) and 1.5 Hz (1st mode clamped on both sides) are reported (Runkel, 1987; Fiedler, 2002; Pohlus and Paquée, 2018). In the upper bearing, the location tolerance of the centering pins limits the maximum amplitude of the cantilevered beam mode. A hard limit for the lateral deflection amplitude of the simply supported modes is the gap between two neighboring fuel assemblies of about 1.6 mm. In case of in-phase motions of neighboring fuel assemblies larger deflections are possible (Pohlus & Paquée, 2018).

During the time in the core, lateral stiffness and natural frequency of the fuel assemblies decrease significantly (Trenty, 1995; Billerey, 2005). Two main mechanisms are responsible for this behavior. Small springs holding the fuel rods in place within the spacer grids relax with neutron flux due to irradiation creep. Consequently, the stabilization of the skeleton by the initially tightly connected fuel rods strongly decreases. This effect is even more distinct for some modern fuel assembly designs, where the springs are not designed as separate parts from stainless steel, but integral parts of the zirconium-based spacers (Wanninger et al., 2016a). A second mechanism is the different irradiation growth (or even shrinkage) of spacer and fuel rods, which increases the gap between the spacer and fuel rods, further reducing the contact force of the spring. The contact force and the friction in the spacers are also responsible for the observed hysteresis in displacement, which significantly contributes to the mechanical damping (Collard, 2004). Consequently, the mechanical damping decreases with time in the core as well.

Fuel assembly oscillations can modulate neutron flux in different ways as they change the moderator/absorber/fuel ratio and distribution, the distance between source and detector, the relative movement in temperature plumes or bypass flows, the motion of the detector in a neutron flux gradient, the reflector thickness at

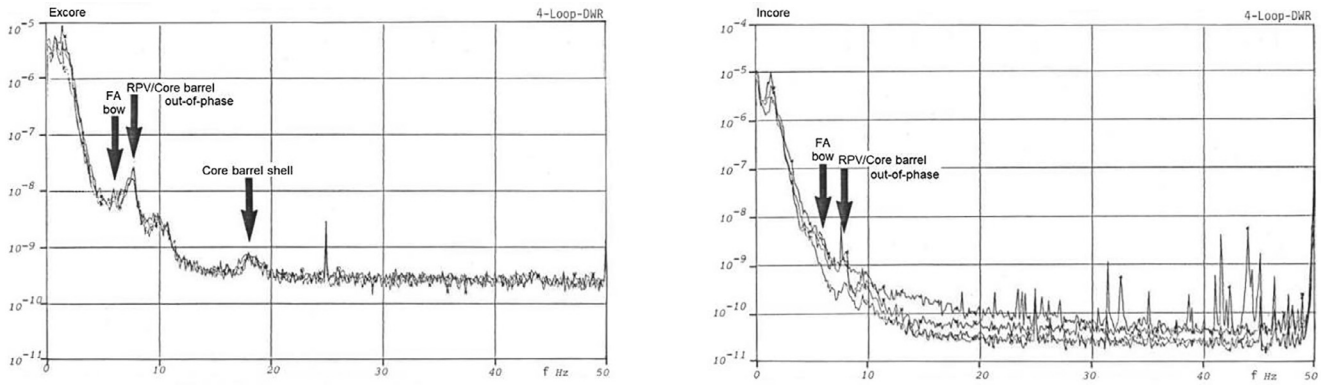

Fig. 1. Exemplary APSD with identified signals associated with component oscillation modes, here: KWU 1300 MW_e class PWR in the period shortly after commissioning (Sunder, 1985).

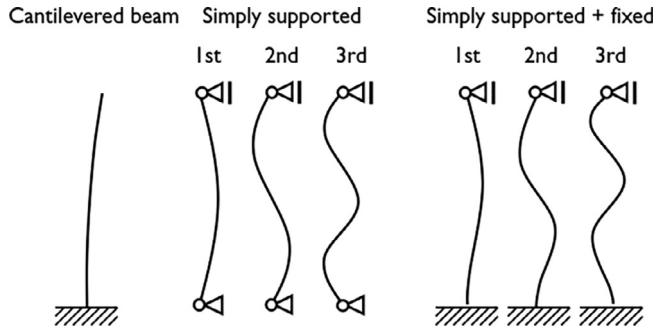

Fig. 2. Idealized fuel assembly oscillation modes.

the core edge or can have indirect effects via thermal hydraulic parameters (Runkel, 1987; Herb et al., 2016). The signals of the uncorrelated motion of the fuel assemblies largely compensate each other in the ex-core detector signals so that a clear identification is usually possible only by in-core detectors. The main identification criterion is an in-phase behavior of sensors at different altitudes (Runkel, 1987; Fiedler, 2002). (Sunder, 1985) concluded that at least the outermost fuel assemblies can be (weakly) seen also in ex-core detectors.

Defects of the fuel assemblies reported in literature encompass e.g. the break of a hold-down spring or the loosening of a guide thimble fixation (Runkel, 1987). Mechanical defects can influence the form, amplitude and frequency of the oscillation. Strong unexpected oscillations involving self-excitation mechanisms were reported e.g. for fuel assemblies of an experimental fast breeder reactor in (Mitzel et al., 1982) and a novel fuel assembly design during a flow-sweep-test in (Haslinger et al., 2001) due to insufficient design.

2.2.2. RPV and core barrel

The RPV and core barrel oscillations can be idealized as pendulum-like oscillators, since the bodies of the components are rather stiff, and the flexibility is concentrated in the upper bearing (Fig. 3). While the RPV is mounted to an external rigid structure via support lugs, the core barrel is mounted to the RPV via hold-down clamps and a supporting plate. Gravity plays only a minor role in the pendulum motion since the energy predominately oscillates between kinetic energy and deformation energy of the bearing. A certain damping comes from the bearing and the fluid in the downcomer (Wach & Sunder, 1977). The coupled system of RPV and core barrel can oscillate in two basic modes: in-phase, with RPV and core barrel swinging in the same direction,

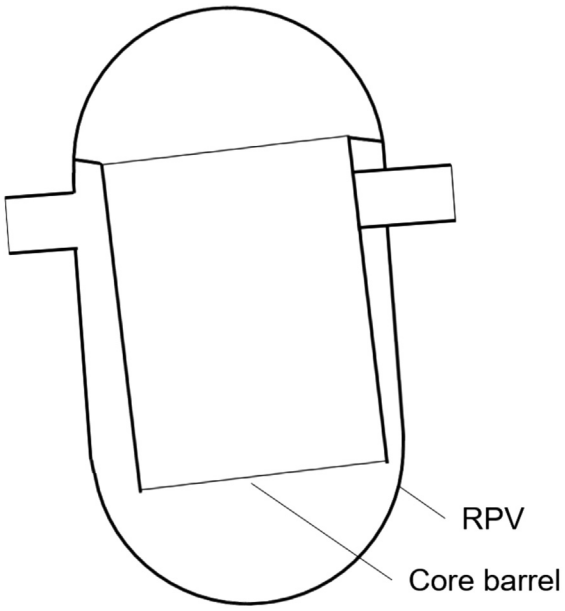

Fig. 3. Schematic representation of the coupled system of RPV and core barrel pendula.

and out-of-phase, with RPV and core barrel swinging in opposite directions. For the out-of-phase mode a natural frequency of 7.4–9.3 Hz is reported for a KWU 1300 MW_e class PWR, which is depending on the oscillation direction as the design and fixation is not uniform. In-phase modes are found in the range of 10.3–12.4 Hz (Runkel, 1987; Fiedler, 2002). The out-of-phase mode is strongly influenced by the fluid in the annular gap. (Altstadt & Weiß, 1999) modelled this effect and calculated natural frequencies of 13.7 Hz vs. 26.3 Hz with/without consideration of the fluid–structure interaction in the annular gap in a VVER.

The RPV further performs vertical oscillations at a frequency of around 14.7 Hz for KWU 1300 MW_e class PWR. The core barrel further performs shell oscillations, which can be separated into shell mode and global mode (Fig. 4). The latter one is more distinct in neutron flux measurements and reported at 18.1–22 Hz for KWU 1300 MW_e class PWR (Runkel, 1987).

The strongest transfer mechanism of the RPV/core barrel oscillations to the neutron flux measurements is the modulation of the reflector thickness in form of the annular gap and its moderation and absorption capabilities (Herb et al., 2016). The change of the distance between source and detector may have an additional,

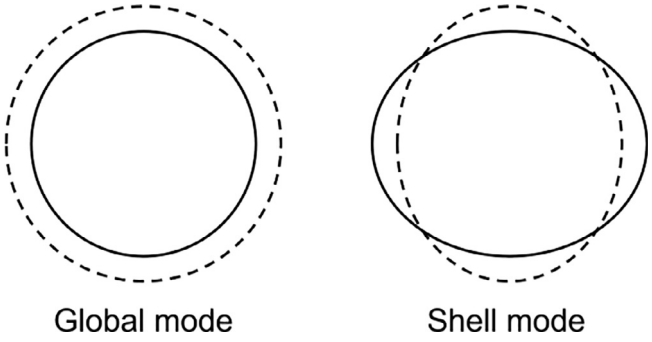

Fig. 4. Schematic representation of the global and shell mode of the core barrel.

but smaller effect (Runkel, 1987). The signal of the in-phase mode is weaker compared to the out-of-phase mode. Via the lower support plate and the upper grid plate, the movements are also transmitted as 'base point excitations' to the fuel assemblies, which themselves have effects on neutron flux measurements of the in-core sensors (Sunder, 1985). During normal operation, when all control rods are pulled out of the core, the RPV vertical mode is not visible in neutron flux measurement.

The identification of a core barrel defect in the Palisades NPP was one of the first applications of neutron flux noise analysis in the field of damage detection (Fry et al., 1974). Further cases of core barrel defects are reported in (Liewers et al., 1988; Damiano and Kryter, 1990; Altstadt and Weiß, 1999; Schumann, 2000). Cases of relaxed hold-down springs or insufficient bolt pre-load resulted in a frequency shift. Cases with a complete loss of fixation resulted in a 'rocking' motion of the core barrel rather than a harmonic oscillation. In this case, collisions with the RPV introduced chaotic aspects into the motion behavior (Liewers et al., 1988).

2.2.3. Further internals with minor or only defect-related effect

The individual fuel rods can be excited to bending oscillations. The mode of oscillation is determined by the distance between the spacers and the bearing therein (Fig. 5). In KWU 1300 MW_e class PWR frequencies of 26–30 Hz have been reported (Fiedler, 2002). The amplitudes are rather small, in the range of 10^{-3} to 10^{-2} of the diameter of the rod (Païdoussis, 2016). The fuel rod oscillations can be regarded isolated from a mechanical point of view, as they are not strongly mechanically coupled to RPV, core barrel or fuel assemblies. A signal is usually only visible in the case of a defect close to an in-core detector (Runkel, 1987). A failure of a single spacer bearing is described in (Sunder, 1985). The failure led to a doubling of the vibrating section length and thus a halving of the corresponding oscillation frequency. A specific kind of flow-induced vibration of fuel rods at the outer core boundary, termed 'Baffle Jetting', historically occurred in reactor designs with a countercurrent flow configuration in the bypass region. Increased gaps between baffle plates and the differential pressure led to jet flows directed radially towards the core. These flows caused vibrations and damage at the outermost fuel rods of the fuel assemblies near the baffle gaps (O'Cain, 2013). The effect is discussed in detail in (Damiano and Kryter, 1990; Fujita, 1990).

Mechanical oscillations of the control elements concern either the components itself or the drive mechanisms. For KWU 1300 MW_e class PWR natural frequencies were reported at 3.5 Hz (1st mode) and 17.5 Hz (2nd mode) (Wehling et al., 1985). During normal operation, when control rods are pulled completely out of the core, no effect on neutron flux can be observed. In special operating conditions with partially inserted control rods, the oscillations modulate the water gap around the absorber and can be clearly observed in in-core and ex-core neutron flux detectors with a coherence of the sensors at different altitudes (Runkel, 1987). Defects of the control elements encompass bearing damages, broken control rod spiders or other broken parts of the component (Damiano and Kryter, 1990; Demazière, 2017). Especially in VVER reactors, cases of excessive flow-induced vibrations were observed leading to mechanical damage (Schumann, 2000). Due to the construction of the control elements as double pendulum configuration and collisions with the walls, the signal showed a chaotic characteristic (Hollstein, 1995).

Fig. 5. Schematic representation of the fuel rod oscillation mode.

Mechanical oscillations of neutron flux instrumentation tubes itself or other instrumentations can be visible in in-core sensors (Runkel, 1987). Cases of specific defects were reported in (Damiano and Kryter, 1990; Païdoussis, 2006). Similar defects were also observed in BWR type reactors (Damiano and Kryter, 1990; Païdoussis, 2006; Demazière, 2017).

In some older PWR, a so-called 'thermal shield' in form of a core-height steel cylinder outside the core barrel is part of the oscillation system RPV/core barrel. It is standing upright on the RPV bottom performing 'wobbling' oscillations where the lower end remains round due to the rigid connection with the RPV and the upper end performs shell-like oscillation (Sunder, 1985). A frequency of 3.2–4.5 Hz is associated with this oscillation in KWU 1300 MW_e class PWR (Runkel, 1987). Common reported defects concerning the thermal shield are the loosening of the component fixation (Damiano & Kryter, 1990) or large-amplitude self-excited oscillations based on the phenomenon of leakage flow in the annular passage (Mulcahy, 1983). The latter effect, involving a periodic interaction between fluid flow and flow passage cross section is described in more detail in (Païdoussis, 2006; Kaneko, 2014).

The upper grid plate and lower support structure hold the fuel assemblies in place. They perform membrane oscillations with possible transmission effects on the fuel assemblies and core barrel (Runkel, 1987).

The purpose of the secondary core support structure in the lower plenum of the RPV is the fall protection for the core barrel and its internals. Under normal operation conditions, the secondary core support has no contact to the core barrel and is fixed only to the RPV. The component performs direction dependent bending and torsional oscillations at 29.3–29.8 Hz, respectively 39 Hz in KWU 1300 MW_e class PWR (Wehling et al., 1985; Fiedler, 2002). It forms a coupled oscillation with the RPV (Runkel, 1987). In newer reactors built by KWU it is replaced by a flow skirt (Fiedler, 2002). Defects of the secondary core support include, among other things, especially loose bolting (Damiano and Kryter, 1990; Stegemann and Runkel, 1995).

2.3. Mechanisms of component excitation

2.3.1. Random fluid field fluctuations

When it comes to the kind of excitation mechanisms, all components listed in section 2.2 are unavoidably excited by random fluctuations of the fluid field, which results in oscillation of the component predominantly at its natural frequencies (Borsoi, 2001; Kaneko, 2014). The causal fluid fluctuations comprise mainly turbulent fluctuations (turbulent buffeting), but also other local inhomogeneous flows. The amplitudes are generally small, and the average vibration amplitude normalized to the characteristic length y_{rms}/L rarely exceeds 10^{-1} (Païdoussis, 1982; Kaneko, 2014). (Laggiard et al., 1995) carried out measurements of components oscillations excited by turbulent buffeting in the 350 MW

Obrigheim plant with special accelerometers. The root mean square (RMS) of the fuel assembly deflection was determined 35 μm. The RMS of the core barrel deflection was determined 27 μm (Laggiard, 1995; Runkel et al., 1997). (Pohlus & Paquée, 2018) made a rough estimation by comparing signals of a single broken fuel assembly with intact fuel assemblies. Due to the fact that the amplitude of the broken fuel assembly was geometrically limited, they were able to estimate the maximum amplitude of an intact fuel assembly as 160 μm with an average variation of about 50 μm. (Fry et al., 1984) reconstructed fuel assembly oscillation amplitudes from ex-core detector neutron noise at Sequoyah 1 PWR. The reconstructed amplitudes could be separated into a correlated part amongst all fuel assemblies of 0.37 μm RMS and an uncorrelated part of 3.1 μm RMS. (Thie, 1981) reconstructed the RMS of the core barrel motion from neutron flux noise signals as 20–60 μm.

2.3.2. Oscillating fluidic forces

Especially prone to oscillating fluidic forces in the form of pressure pulsations from outside the RPV are the pendulum and the shell mode of the core barrel (Wach & Sunder, 1977). This makes it possible to detect further effects indirectly in neutron flux measurements, which are transferred via fluid pressure. The response to pressure pulsations can be especially amplified when the excitation frequency is close to a natural frequency of the oscillation modes (Runkel, 1987).

Mechanical vibrations of primary circuit components can be transmitted via the fluid and via the structure. The most significant of these is the natural vibration of the steam generators at about 1 Hz (Bauernfeind, 1988; Wach and Sunder, 1989). (Wehling et al., 1985) listed numerous further oscillation modes of primary circuit piping and components. (Stegemann & Runkel, 1995) found even ground motions caused by neighboring aggregates in neutron flux signals.

A strong excitation force comes from remaining imbalances of the main coolant pump. The effect can be identified as sharp peak in the APSD of both in-core and ex-core neutron flux signal at a divisor of the power frequency due to the design of the pumps as induction machines (between 24.8 and 25 Hz and at 12.5 Hz for 50 Hz line frequency) (Runkel, 1987; Fiedler, 2002). The strong signal allows it to detect irregularities in the pump function, such as large imbalances, cracks in the pump shaft and bearing damages (Stegemann and Runkel, 1995; Altstadt et al., 1997) or oscillations in the motor supply current (Stulík et al., 2019). A further effect stemming from the main coolant pump concerns acoustic pressure pulsations from passing pump blades at high frequencies (Banyay et al., 2013).

2.3.3. Vortices

A hypothetic type of excitation encompasses the intrusion of perturbations, i.e. vertices, into the core. (Altstadt et al., 1997) postulated a vortex forming in a VVER when the fluid is deflected into the downcomer at the end of the inlet nozzle. A detachment frequency of 0.92 Hz was calculated. However, the calculated lifetime of the vortex raises doubts whether it would reach the core.

In some Westinghouse 4-loop plants, a phenomenon known as ‘lower plenum anomaly’ has been observed. This describes a stationary vortex in the lower plenum which affects the mass flow profile at the core inlet and locally excites fuel assembly clusters (Conner et al., 2003).

Independent of the frequency of the vortex rotation and vortex sequence, a characteristic frequency is represented by the reciprocal of the time between the fluid entering and leaving the core, which in KWU 1300 MW_e class PWR is 4.3 m/s divided by 4.9 m, leading to a characteristic frequency of 0.87 Hz.

2.3.4. Fluid-elastic mechanisms in the cooling loop

A fluid-elastic oscillation phenomenon, which can be also indirectly observed in all neutron flux measurement signals and especially in pressure transducers, concerns standing waves (Sunder, 1985; Fiedler, 2002), see Fig. 6. The frequency of the waves depends on the length of the channel and the configuration of its ends. When the average coolant temperature decreases, the frequencies shift upwards according to the increase in the speed of sound making them distinguishable from pressure pulsations induced by component vibrations (Runkel, 1987). (Runkel 1987; Fiedler 2002; Seidl et al., 2015) listed corresponding peaks in the pressure transducer APSD signal, starting from 5.3 Hz.

Unexpected gas volumes in the RPV may initiate a cavity resonance oscillation, which modulates neutron flux in the core via a global reactivity effect (Runkel, 1987; Fiedler, 2002). A cavity resonance is characterized by an oscillation of energy between pressure in the cavities and kinetic energy of the fluid (Fig. 7). (Fiedler, 2002) attributed a signal in the pressure transducers of a KWU 1300 MW_e class PWR at around 0.5–1 Hz to a hypothetical cavity resonance between the pressurizer gas volume and an unidentified gas volume in the RPV, possibly subcooled boiling. The signal showed an in-phase behavior between all sensors. The amplitude was higher for the loop encompassing the pressurizer. A signal around 7.5 Hz is sometimes attributed to a cavity resonance as well (Runkel, 1987; Seidl et al., 2015).

In (Grunwald et al., 1982), a fluid-elastic oscillation between the upper and lower plena of the RPV was assumed to occur in a VVER, with the hydraulic resistance of the core postulated to be infinite (Fig. 8). In this mode of oscillation, the restoring force is not due to a volume of gas, but to the elasticity of the vessel and pipe walls. The frequency could be calculated analytically as 0.5–0.9 Hz. The oscillations of the six loops were assumed to overlap in an uncorrelated manner. Similar mechanisms could be hypothesized between other communicating vessels, e.g. opposite loop pairs.

2.3.5. Fluid-elastic and self-excited mechanisms in the core

During the search for underlying physics of the increased neutron flux noise in KWU 1300 MW_e class PWR (see chapter 1), a collective motion of the entirety or large groups of fuel assemblies was frequently discussed (Seidl et al., 2015). In its simplest form, the collective motion was interpreted as a reaction to a postulated oscillating mass flow inlet, figuratively represented by seagrass following seawater fluctuations. Looking deeper, this neglects that the motion of the volume of the fuel assemblies displaces and deflects a significant amount of water and therefore has a reactive effect on the fluid field. This effect could be well observed in investigations on static fuel assembly deformations (Paramonov et al.,

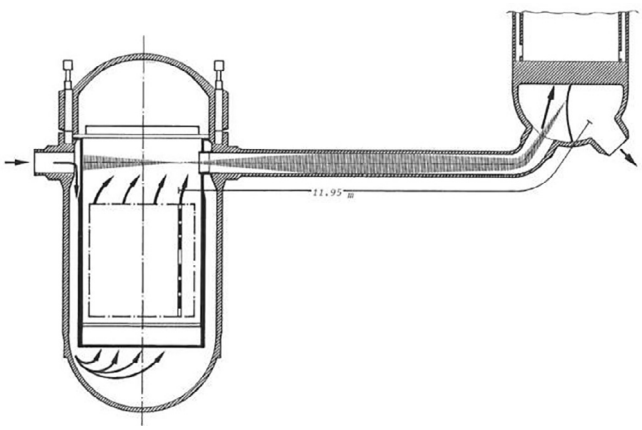

Fig. 6. Standing wave between RPV and steam generator (Sunder, 1985).

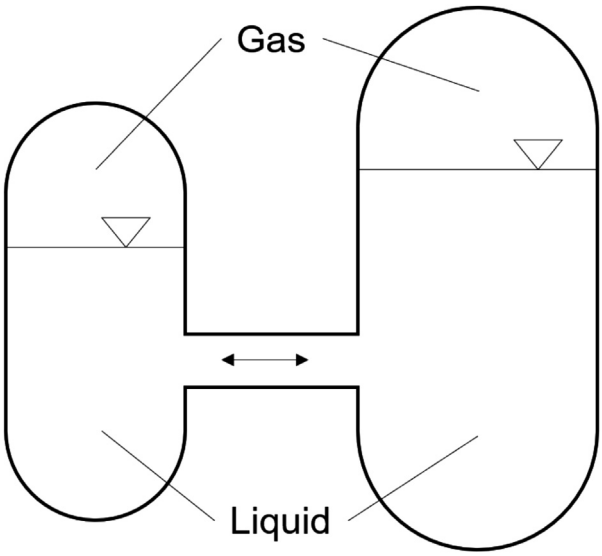

Fig. 7. Schematic representation of a cavity resonance oscillation following the description of (Fiedler, 2002).

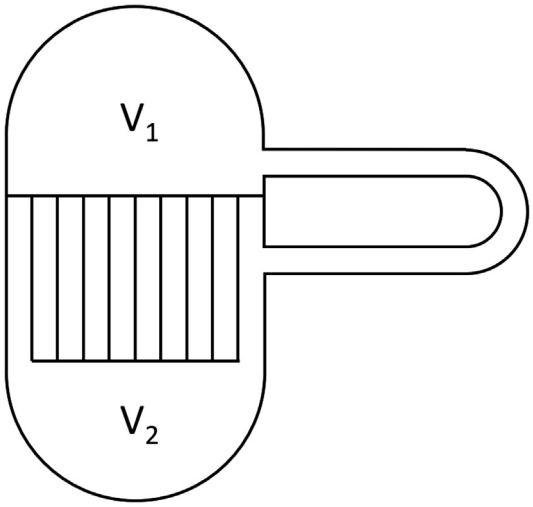

Fig. 8. Schematic representation of a suspected fluid-elastic resonance following the description of (Grunwald et al., 1982).

2001; Conner et al., 2003). Considering this, the fuel assemblies and the fluid in a half or a local area of the core should be seen as a complex oscillator, where the proportion of fuel assembly volume to water volume and the fluid mass flow periodically changes (Fig. 9).

In KWU plants with a flow skirt in the lower plenum, the noise level was observed significantly lower, presupposing that the flow skirt modifies this global oscillation, e.g. by introducing additional damping (Herb et al., 2018). In particular, it remains unclear, whether random fluctuations are sufficient to excite this oscillation or whether an oscillating external excitation force (as described in previous subchapters) is necessary as a driver. A self-excitation of the oscillator of the system of fluid and structure could be taken into account as well, similar as it has been reported in the past for annular flows inside the RPV in conjunction with a thermal shield (Blevins, 1979; Chen, 1983; Mulcahy, 1983; Axisa, 1993; Païdoussis, 2006; Kaneko, 2014).

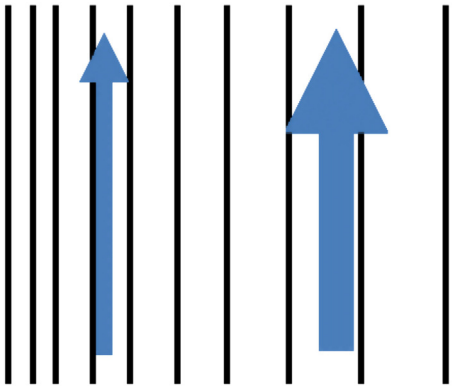

Fig. 9. Visualization of a global vibration encompassing fuel assemblies and fluid.

3. Mechanical model of the RPV internals dynamic behavior

3.1. Literature background

Models for the simulation of the dynamic motion behavior of RPV internals are described in literature for various purposes and in various detail. Models for single and multiple fuel assemblies have been used e.g. for seismic analysis or the assessment of flow induced vibrations (Fontaine and Politopoulos, 2000; Broc et al., 2003; Viallet and Kestens, 2003; Collard, 2004). Some consider internal mechanical processes such as contacts and friction, others include reactive forces and coupling effects of the surrounding fluid, e.g. by means of added mass, stiffness and damping values, porous media or other approaches (Ricciardi et al., 2009b; Ricciardi, 2016). Models of the RPV and core barrel have been e.g. used to evaluate flow induced vibrations from turbulence in the downcomer annular gap (Snyder, 2003; Palamera, 2015; Wei, 2015).

The idea of generating mechanical models of RPV internals for the specific purpose of identifying and interpreting measured oscillations, e.g. in neutron flux, and assigning them to normal and anormal component conditions goes back to (Bauernfeind, 1977). He generated a simple mechanical model comprising RPV, core barrel (including core) and secondary core support (Fig. 10). In his work, model parameters were determined by tuning them to

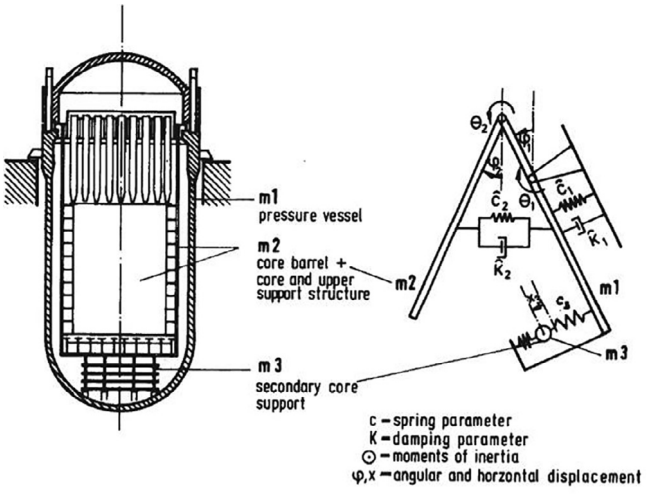

Fig. 10. Model of the mechanical coupling of RPV and core barrel according to (Bauernfeind, 1977).

natural frequencies found during pump shutdown tests. Other parameters were obtained from manufacturer's data. In (Bauernfeind, 1988) primary circuit components were added. Similar models were developed for PWR by (Wach & Sunder, 1977) and for VVER by (Dach et al., 1985) and (Altstadt & Weiß, 1999). The model presented in the following subsections, which is implemented in the code ANSYS Mechanical (ANSYS Inc., 2019), is based on the idea of (Bauernfeind, 1977) and extends these kinds of models by a representation of a row of fuel assemblies and a consideration of reactive fluidic effects.

3.2. Model of a single fuel assembly

3.2.1. Model setup

Fig. 11 shows the mechanical model of a single fuel assembly. The structure is represented by a single bending beam fixed in all translational dimensions at the bottom and in horizontal direction at the top. Internal structures are not resolved and longitudinal growth due to irradiation is neglected. The weight is evenly distributed over the length l_{FA} by choosing appropriate values for cross-section area A_{FA} and density ρ_{FA}. All area moments of inertia except the one responsible for bending in the paper plane I_{yy} are chosen sufficiently stiff. The beam is discretized into a sufficient number of finite elements, which is checked by a mesh study.

The product of Young's modulus E and area of momentum I_{yy} is iteratively adapted to achieve a specific lateral stiffness of the fuel assembly. Tuning of mechanical parameters to measured data is a common practice for mechanical models of RPV internals (Altstadt et al., 1997; Jeon et al., 2009). Optionally, the stiffness can be partially attributed to the torsional spring c_{rot} to obtain more realistic deflection shapes, measured e.g. in (Jeon et al., 2009; Ricciardi, 2016; Wanninger et al., 2016b), which is not used for the moment.

Volume forces from gravity and buoyancy are neglected due to their comparably small size. An appropriate hold-down force $F_{FA,hd}$ is applied, neglecting the relaxation of the hold-down spring forces during the time in the core in a first approach. Axial hydraulic forces arising through the hydraulic flow resistance of spacers and other structural parts ($F_{FA,h}$, $F_{FA,s}$, $F_{FA,f}$) are considered using design values. Permanent lateral hydraulic forces are neglected, since the influence on oscillatory behavior is low when collisions between fuel assemblies are not considered. Damping D_{FA} relative to the environment is attributed to the fuel assemblies, here symbolized by two damping elements.

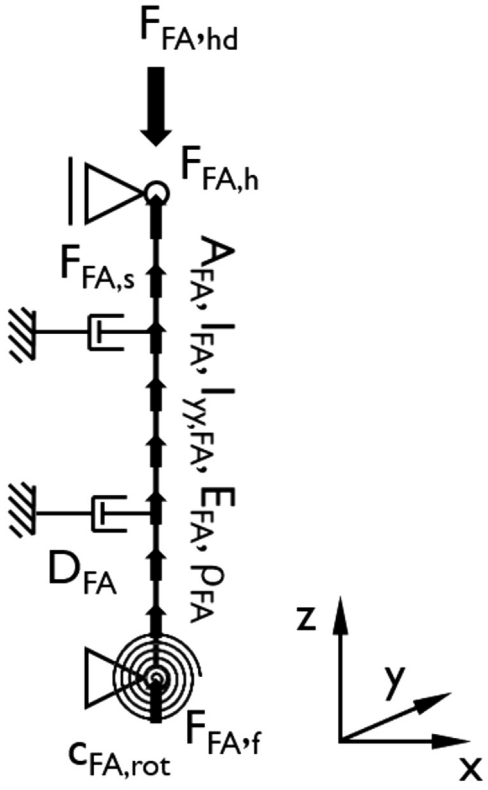

Fig. 11. Model of a single fuel assembly.

3.2.2. Determination of mechanical parameters

For the determination of the lateral stiffness of the fuel assemblies, a literature review has been carried out (Fig. 12). The shown values refer to a deflection from a single force in the middle of the fuel assembly. The collected data can be divided into three groups. The first group can be associated with various traditional fuel assembly designs. A special characteristic is the bilinear course of the stiffness with different values for deflections below and above about 4 mm. The next group can be associated with some modern fuel assembly designs, especially Areva High Thermal Performance (HTP) (Areva Inc., 2010). The stiffness decreases significantly between beginning of life (BOL) and end of life (EOL) due to relaxing fixation springs and decreasing contact forces between spacer and fuel rods and irradiation growth (Billerey, 2005). The last group describes data of fuel assembly skeletons without fuel rods. Based on these data, three generic kinds of fuel assemblies are determined. The first one with 150 N/mm represents conventional fuel assemblies for small deflections. The second and third with 60 N/mm and 30 N/mm represent modern fuel assembly types with their pronounced decrease in lateral stiffness between BOL and EOL. For validation, modal analyses of the first (3.0 Hz; 1.9 Hz; 1.4 Hz) and second (11.5 Hz; 7.6 Hz; 5.6 Hz) mode have been conducted and successfully compared to literature data in), (Fry et al., 1984; Runkel, 1987; Bauernfeind, 1988; Fontaine and Politopoulos, 2000; Fiedler, 2002; Viallet and Kestens, 2003; Billerey, 2005; Pohlus and Paquée, 2018).

Mechanical damping phenomena of the fuel assemblies include material damping, damping in the screwing as well as frictional damping and damping from deformation hysteresis, the latter being the main contribution (Viallet and Kestens, 2003; Collard, 2004). Collisions of fuel assemblies may further involve squeeze-film damping (Pettigrew et al., 1998). A survey on available data on pure mechanical damping without fluidic effects, which have been measured in context of seismic analyses, revealed values mostly below D = 0.15, especially for low and moderate amplitudes (Pettigrew, 1998; Pisapia et al., 2003; Viallet and Kestens, 2003; Lu and Seel, 2006). Analogue to the decrease of stiffness with time,

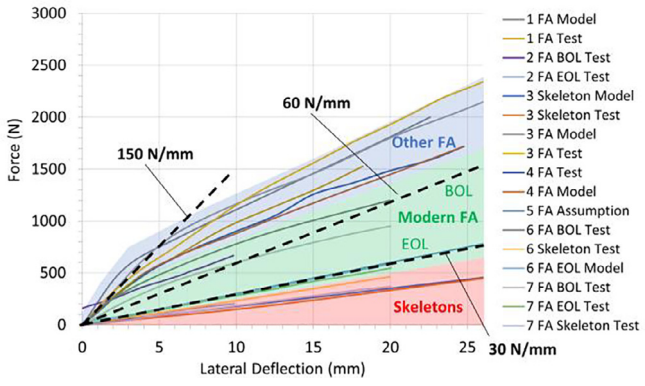

Fig. 12. Fuel assembly lateral stiffness in 1: (Fontaine & Politopoulos, 2000), 2: (Collard, 2004), 3: (Jeon et al., 2009), 4: (Morales et al., 2012), 5: (Horváth & Dressel, 2013) and 6: (Wanninger et al., 2016b), 7: (Wanninger, 2018).

mechanical damping may undergo a decrease during the time in the core as well, as a major part stems from the hysteresis between deflection and deflection force, which decreases with relaxing fixation of the fuel rods in the skeleton.

3.2.3. Representation of reactive fluidic forces

Reactive (secondary) fluidic forces, which are caused by the oscillator motion itself, can be included in a linearized manner in terms of added mass, added damping and added stiffness, visualized by transforming Eq. (1) to Eq. (2) where m_s is the real and m_{fs} the added mass, c_s is the real and c_{fs} the added damping, k_s is the real and k_{fs} the added stiffness, x the oscillator position, t the time, f_t the sum of the external excitation forces and f_{fs} of the reactive fluidic forces.

$$m_s * \ddot{x}(t) + c_s * \dot{x}(t) + k_s * x(t) = f_t(t) + f_{fs}(\ddot{x}, \dot{x}, x) \quad (1)$$

$$\left[m_s + m_{fs}\right] * \ddot{x}(t) + \left[c_s + c_{fs}\right] * \dot{x}(t) + \left[k_s + k_{fs}\right] * x(t) = f_t(t) \quad (2)$$

The size of the added values is not a fixed property of the system, but significantly depends on the type of excitation and boundary conditions (Stabel and Ren, 2005). The fluid-induced added damping e.g. significantly depends on whether there is a relative motion between fuel assemblies and surrounding fluid or whether the fuel assemblies are moving together with the oscillating fluid. Added mass and stiffness have been further shown significantly dependent on the confinement of the flow. For self-induced oscillations even negative added values could arise. Therefore, the values are left undefined in the mechanical model and parametric studies are conducted to cover the complete range of the model dynamic behavior.

To have a set of comparative values, literature data from shaker table tests on single fuel assemblies in axial flow and corresponding calculations are reviewed, which have been done in conjunction with seismic analysis (Rigaudeau et al., 1993; Viallet and Kestens, 2003; Pisapia et al., 2003; Collard, 2004; Ricciardi and Boccaccio, 2015; Ricciardi, 2016; Ricciardi, 2017). Depending on boundary conditions, the added mass differed between -20 % and +60 % of the structural mass and the added stiffness between -30 % and +5 % of the structural stiffness. The finding that for real fuel assemblies natural frequencies in constant axial flow differ by only around factor 0.9 from the value measured in air further strengthens the presumption that in practice added mass and stiffness have only a limited effect on dynamic properties (Sunder, 1985; Pisapia et al., 2003; Ricciardi, 2016).

The main components of fluidic damping are viscous damping of the surrounding fluid and flow-dependent damping. While the first one is caused by drag effects and can be already observed in still fluid, the latter arises from a lift phenomenon due to axial flow velocity relatively to the assembly lateral velocity (Viallet & Kestens, 2003). Data on fluidic damping, which has been obtained from shaker table tests and corresponding calculations, done in conjunction with seismic analysis, is shown in Fig. 13.

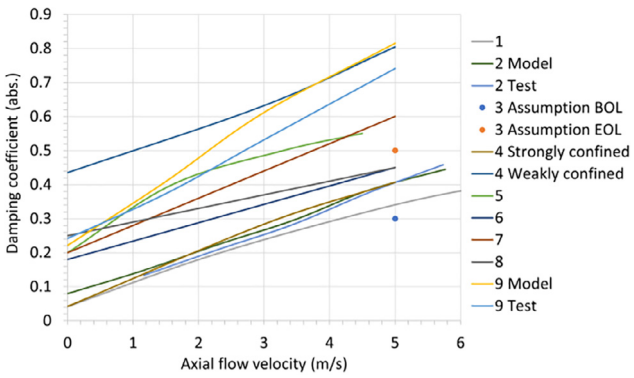

Fig. 13. Fluidic damping of fuel assemblies in axial flow in 1: (Fujita, 1990), 2: (Shah et al., 2001), 3: (Viallet & Kestens, 2003), 4: (Pisapia et al., 2003), 5/6/7/8: (Lu & Seel, 2006), 9: (Ricciardi, 2016).

3.3. Model of the full system of RPV and internals

The full model encompasses RPV, core barrel and fuel assemblies, since oscillations of these components have been found among the main sources of geometry noise in PWR during normal operation (see section 2). For simplification, the number of fuel assemblies is reduced to one row of 15 fuel assemblies. The model of the fuel assemblies is described in section 3.2. To keep the coupling characteristics and the momentum exchange realistic, the weight of all 193 fuel assemblies is distributed over the single row, adapting the other parameters to keep the dynamic behavior the same. The underlying assumption for this simplification is that the motions are either uncorrelated, and in this case the behavior of one row is representative for the whole core, or the motions are correlated, and in this case the correlated motion is approximately symmetric anyway.

RPV and core barrel are represented by stiff beams, mounted pivoted to a fixed structure (Fig. 14). The structural weight is distributed homogeneously. At the bottom of the core barrel, an additional point mass is attached, representing the mass of additional structural parts. In a first approximation, the weight of the water content and the displaced water is added to the structure. The fixation of the RPV to the environment is represented by a spring element, neglecting the damping in this connection. The mounting of the core barrel to the RPV and the fluid–structure interaction in the annular gap is modelled by a further combined spring and damping element, see (Bauernfeind, 1977). The beams are discretized into a sufficient number of finite elements, which is checked by a mesh study.

The spring stiffness k_{RPV}, the spring stiffness k_{CB} and the damping D_{CB} are determined based on natural frequencies (Runkel, 1987; Fiedler, 2002), the preliminary work of (Bauernfeind, 1977) and (Wach & Sunder, 1977) as well as considerations regarding fluid–structure interaction in the annular gap in (Altstadt & Weiß, 1999) and (Yun Je et al., 2017). The row of 15 fuel assemblies with characteristics according to section 3.2 is attached to the core barrel with axial offset from the bottom. To represent the fluidic near field coupling between adjacent fuel assemblies, further spring elements are attached.

In the reactor situation, the fuel assemblies are coupled among each other by fluidic and mechanical mechanisms. A fluidic near-field coupling comprises inertial and dissipative effects that

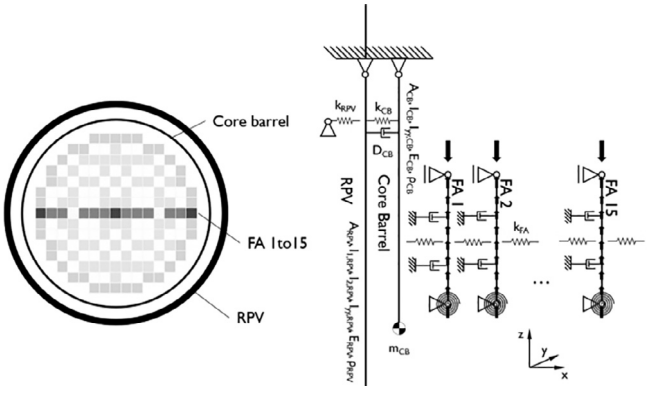

Fig. 14. Model of the full system of RPV and internals.

change the surrounding pressure and velocity field near the oscillator. Literature data conclude that the fluidic near-field coupling is either negligible (Fry et al., 1984; Rigaudeau et al., 1993) or moderate (Broc et al., 2003; Witters, 2004; Ricciardi et al., 2009a). Although not enough quantitative data is available to determine a specific value, the coupling effect can be investigated by a parametric study. A far field coupling, which is not considered here, may further arise e.g. from the redistribution of the fixed mass flow over different channels or an indirect coupling via the core baffles, which was proposed by (Rigaudeau et al., 1993). The mechanical coupling is mediated via the interconnections between the components. A further mechanical coupling stems from collisions among fuel assemblies and between the outer row of fuel assemblies and the core baffle. It will get relevant, when the motion of the fuel assemblies exceeds the width of the gap of approximately 1.6 mm (Pohlus & Paquée, 2018). Collisions and contacts will introduce a non-linearity into the system. The consideration of collisions is therefore postponed to future work.

4. Application of the mechanical model to generic excitation scenarios

4.1. Applied excitation scenarios and model parameters

The possible sources of RPV internal excitations encompass a wide field of known and hypothetical phenomena (see chapter 2). These can be of fluidic or mechanical nature, predominantly evoked by external force, inertia or relative velocity to the surrounding fluid and may be either modulated by an external source or building an oscillator on their own. As the underlying effect of the observed rise in neutron flux noise (see chapter 1) is unknown yet, an appropriate approach is to apply different generic excitation scenarios to the model and conduct parametric studies to learn more about the general behavior of the system and be able to explain observations and to narrow down hypotheses. Therefore, the following forced excitation scenarios are applied. Stochastic, seismic and self-induced excitations are not considered in this stage.

- Correlated sinusoid excitation of all FAs with 20 N per FA at 1 Hz
- Correlated sinusoid excitation of all FAs with 200 N per FA at 1 Hz
- Local sinusoid excitation of 3 of 15 FAs at the core edge with 200 N per FA at 1 Hz
- Shifted sinusoid excitation of all FAs with $200N * sin(2\pi * (1Hz * t + n/15))$ per FA, with n = FA position
- Sinusoid excitation of the core barrel and (in anti-phase) the RPV with 30 kN at 1 Hz

The frequency of 1 Hz is chosen within the magnitude of the effect observed in KWU 1300 MW_e class PWR to determine the system response in this region. The size of the applied force amplitude is chosen in a range, where a significant deflection is expected, although it has only quantitative influence on the system response due to the system's linearity. A force of 20–200 N is able to deflect a single FA in the millimeter range. For the application to the model, which includes only one row of FAs, it was scaled up accordingly. A force of 30 kN is taken from calculations of forces in the downcomer that stem from vortices and main coolant pump pulsations large enough to excite the RPV and core barrel to motions visible in the neutron flux measurement (Altstadt et al., 1997; Zeman and Hlaváč, 2008). For each excitation scenario, studies with different parameters are conducted:

- Fluidic damping of the individual FAs either neglected or set to D = 0.5.
- Fluidic near field coupling between FAs/core barrel either neglected or set to k = 150 N/mm.
- FA loading pattern either homogeneous (150 N/mm lateral stiffness) or heterogeneous (alternately 150 N/mm, 60 N/mm and 30 N/mm).

The fluidic damping is chosen as an average of the literature values in seismic analyses (Fig. 13). The value for near field coupling is chosen in the range of the FA stiffness, where an influence would be expected. The heterogeneous loading pattern represents a mixed core with fresh and older FAs or FAs of different type.

4.2. Resulting motion trajectories

While all combinations of excitation scenarios and parameters have been investigated, Fig. 15 shows some selected results of the component reactions with assignments to excitation scenarios and parameters given in Table 1. The plots represent the time history of the horizontal component position at mid height level of the FAs, assuming that the oscillation mode is of C-shape for the FAs and pendulum-like for core barrel and RPV. In the upper part of the diagram, the responses of the FAs are depicted with a distance between each other that approximately corresponds to the gap between FAs in the reactor. In the lower part, the response of the RPV and the core barrel can be seen in an arbitrary distance to each other and the FAs. The amplitude of RPV and core barrel is magnified by factor 10,000 for visualization.

Fig. 15a shows the oscillatory response of the RPV internals to a correlated sinusoid excitation of all FAs in a heterogeneous loading pattern with 200 N amplitude at 1 Hz with damping and fluidic coupling enabled as a first scenario. Although of different stiffness, the FAs perform almost uniform oscillations except for the outermost positions, which are coupled to the much stiffer core barrel via the fluidic near field coupling, which decreases their vibration amplitude. The core barrel reaction shows a slight phase-shift and an amplitude, which accounts for only about 1/2000 of the amplitude of the FAs. The amplitude of the RPV is even lower (about 1/12 of the core barrel) due to its rigidity and the fact that it is not directly coupled to the FAs. The same simulation with an excitation amplitude of 20 N instead of 200 N (graph not shown) reveals an amplitude response of exactly 1/10 size due to the linearity of the system. A non-linearity and a dependence on the force amplitude may be seen when collisions between neighbor FAs and the core barrel/core shroud would be taken into account.

When comparing the first scenario results to those of the same excitation case, but without fluidic coupling (Fig. 15b), it can be seen that the homogenization of the response amplitude vanishes and each FA shows an amplitude according to its lateral stiffness.

When comparing the first scenario results to those of the same excitation case, but without FA damping (Fig. 15c) it can be seen that damping suppresses individual mechanical motions of the components, that otherwise lead to a non-periodic motion pattern.

When looking at the amplitude response to a local excitation (Fig. 15d), it could be seen that the oscillation does not spread over the whole core by fluidic near field coupling or by the mechanical coupling via the core barrel. The observation is the same for simulations without damping (graph not shown).

In the amplitude reaction to a shifted sinusoid excitation (Fig. 15e) it can be seen that the core barrel is only excited when the forces acting on the FAs do not compensate each other and result in a non-zero net reaction force.

The case of an excitation of the RPV/core barrel instead of the FAs (Fig. 15f) shows that this excitation has low effect on the FA amplitudes, since the core barrel reaction amplitude is rather low.

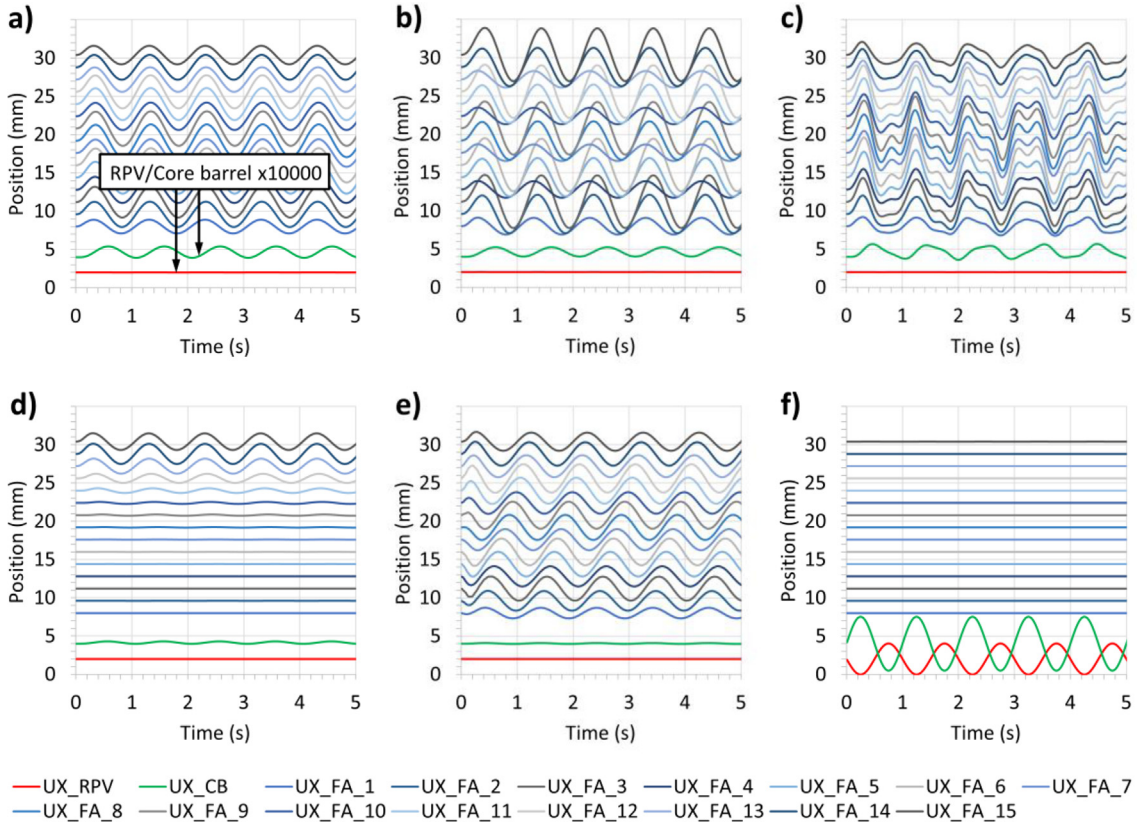

Fig. 15. Patterns of component oscillation from different excitation scenarios and parameter sets, response of RPV and core barrel scaled by factor 10,000.

Table 1
Key to Fig. 15.

Run	Excitation mode	Excited component	Amplitude	Damping	Coupled	Pattern
a)	Correlated sinusoid	Row of all 15 FAs	200 N	Yes	Yes	Heterogeneous
b)	Correlated sinusoid	Row of all 15 FAs	200 N	Yes	No	Heterogeneous
c)	Correlated sinusoid	Row of all 15 FAs	200 N	No	Yes	Heterogeneous
d)	Local sinusoid	3 FAs at corner	200 N	Yes	Yes	Heterogeneous
e)	Shifted sinusoid	Row of all 15 FAs	200 N	Yes	Yes	Heterogeneous
f)	Sinusoid	Core barrel/RPV	30 kN	Yes	Yes	Heterogeneous

4.3. Discussion of the simulation results

When interpreting the resulting motion trajectories, several findings could be made. A postulated fluidic near-field coupling can equalize the FA reaction amplitudes within a certain region regardless of the FAs individual stiffness. This is an explanation for the observed correlation of the neutron flux noise level to the overall share of new-type FAs in the core, rather than to the type, age and stiffness of only the outermost FAs, which can be predominantly seen in the ex-core detectors according to (Sunder, 1985).

In case of a postulated purely mechanical oscillation of the FAs in an otherwise unaffected axial fluid flow, fluidic damping would continually withdraw significant energy from the (mechanical) oscillation of the FAs. Unlike in the seismic case, there is no other way to resupply this energy to the mechanical oscillators than by the fluid itself, as the coupling to the core barrel is weak. This means that the fluid must be part of the excitation and part of the observed oscillation phenomenon. Considering only reactive fluidic effects in the model is therefore not sufficient.

The scenario without damping shows that the observed non-periodic, partly chaotic, signal might stem from a superposition and interaction of several oscillators. In this case, the oscillation of the FAs in the core is not perfectly uniform, but (groups of) FAs with a different oscillation state exist side by side, although the predominant motion is an oscillation between the core halves. Fuel assemblies with decreased damping properties could favor this behavior.

A local excitation source does not spread or synchronize instantaneously core-wide by fluidic near-field coupling or by the mechanical coupling of the core barrel. From the view of the authors, it is further questionable if collisions between FAs or other not yet considered coupling phenomena could be strong and fast enough to spread local phenomena instantly over the whole core. This indicates that either the excitation effect of the phenomenon has the size of the core or the entirety of FAs and the water in between behave as one single oscillator.

The transfer of RPV/core barrel motions to FA motions only via mechanical contacts is weak. The core barrel vibrations observed in the in-core detectors (Sunder, 1985) might have been transported also by other effects. Therefore, a neglection or separate consideration of the RPV/core barrel in future models regarding mechanical coupling may be justified for certain kinds of investigations.

The transfer of FA motions to the RPV/core barrel is weak as well and only apparent if there is a non-zero net reaction force.

The motion of the RPV and core barrel requires a large force, which can be only delivered by pressure oscillations in the annular downcomer working like a hydraulic actuator due to the large surface area of the components.

Overall, the findings affirm that core-wide oscillations of the fluid flow leading to a simultaneous oscillation of individual FA groups, possibly with the influence of bidirectional effects between fluid and structure, in combination with changes of fuel assemblies' mechanical properties, might be responsible for the temporary increase of neutron flux fluctuations observed in KWU 1300 MW_e class PWR.

5. Reduced order modelling of core internals

The investigation of the mechanical vibrations of core components is one part of the necessary research to understand the neutron noise signal inside power reactors. Another part is the transfer of the results of the previous sections to full core investigations including a simulation of the neutron kinetics and thermal hydraulics of the core. A modelling approach of the coupling mechanism between the mechanical oscillations and the neutron noise signal of the neutron detectors is needed to form hypotheses on the causes of any of the observed features in the neutron noise.

In the present article, a modified version of the nodal, diffusion, time-domain, reactor dynamics code DYN3D (Rohde et al., 2016) is applied for the simulation of the thermal-hydraulics, the heat-transfer, and the neutron kinetics inside the core including all relevant feedback mechanisms. This code is coupled to a model of the mechanical vibrations of the core components which was described in Section 3.3. The modifications of the code consider the elongations of the fuel assemblies by using a custom cross section library created with CASMO5 (Studsvik Scandpower Inc.). This library is parametrized such that it respects the time dependent change of the average water gap between the fuel assemblies. This approach builds upon previous research with DYN3D and was already successfully applied to neutron noise investigations in (Viebach, 2019, 2020). In these articles, the effects of a collective motion of all fuel assemblies on the reflector as well as the effect of generic vibrations of the fuel assemblies throughout the whole core were studied. The applicability of DYN3D for neutron noise simulations was investigated in (Viebach et al., 2022). The aim of this section is to use a more realistic model for the mechanical components and apply it to investigate a scenario, where no wide-area collective movement by a strong coupling of the fuel assemblies is presumed. The shown studies are qualitative in nature and focus on the influence of fuel assembly vibrations, exclusively. The neutron noise signal is a collection of many different effects. The investigations at hand thus look at a part of the whole phenomenon, apart from testing the coupling of the mechanical model to the neutronics.

The computational effort of coupled simulations of neutron kinetics and the mechanical model makes it time consuming to conduct parameter studies. Therefore, a model order reduction technique was applied to the mechanical model to reduce the computational effort, while preserving selected characteristics of the model with a well-defined precision. The mathematical basis of this method will be described in section 5.1. The mechanical model and the application of the reduced order modelling will be detailed in section 5.2 followed by a brief description of the modified version of DYN3D in section 5.3. Results with respect to the studied scenario are presented in section 5.4.

5.1. Model order reduction

Model order reduction is a collection of mathematical methods aiming at a reduction of the modelling complexity of a problem whilst retaining certain aspects of the dynamics (Antoulas et al., 2001; Baur et al., 2014). The mathematical foundation of these methods is based on the description of the time-evolution of the state variables $\boldsymbol{x}(t)$ (or the degrees of freedom) in terms of a differential equation:

$$\frac{\mathrm{d}\boldsymbol{x}(t)}{\mathrm{d}t} = \boldsymbol{F}(\boldsymbol{x}(t), t, \boldsymbol{\gamma}) \tag{3}$$

In Eq. (3), $\boldsymbol{\gamma}$ designates a vector of parameters describing an operational point and $\boldsymbol{F}$ is a vector field in phase space. For simplicity, Eq. (3) is restricted to the case of a system of ordinary differential equations, since it is assumed that the underlying system of partial differential equations is discretized.

If the model is sufficiently complex, as is the case for time-domain investigations of nuclear power reactors, the dimension of the state space can be very large, thus leading to very time-consuming computations. This is especially true for wide-range parameter studies or qualitative investigations, such as stability analysis and bifurcation analysis. It is therefore desirable to reduce the number of the degrees of freedom of the mathematical model by neglecting non-essential parts of the dynamics, for example rapidly decreasing components or parts of the dynamics in a frequency range not important to the investigation at hand, like high frequency components in a long-term study. The result of the reduction is an approximative and much smaller dynamical system, called reduced order model (ROM). It is described by a system of new differential equations of the same form, but with a much smaller dimension than the original system in Eq. (3):

$$\frac{\mathrm{d}\,\tilde{\boldsymbol{x}}(t)}{\mathrm{d}t} = \tilde{\boldsymbol{F}}\left(\tilde{\boldsymbol{x}}(t), t, \boldsymbol{\gamma}\right) \tag{4}$$

The various model order reduction techniques differ in the exact process of how to transform Eq. (3) into Eq. (4). For an important class of MOR-techniques, the state vectors are transformed via a simple linear transformation by a matrix $\mathbf{V}$, henceforth called matrix of modes, according to

$$\boldsymbol{x}(t) \approx \mathbf{V}\tilde{\boldsymbol{x}}(t) \tag{5}$$

A real reduction in dimension is only achieved if the number of rows of $\mathbf{V}$ is (much) larger than the number of its columns. The vector field $\boldsymbol{F}$, forcing the dynamics, is transformed with the additional help of a weight matrix $\mathbf{W}$, with $\mathbf{W}^{\mathrm{T}}\mathbf{V} = \mathbf{Id}$ ($\mathbf{Id}$ being the identity matrix), such that

$$\tilde{\boldsymbol{F}}\left(\tilde{\boldsymbol{x}}, t, \boldsymbol{\gamma}\right) := \mathbf{W}^{\mathrm{T}}\boldsymbol{F}\left(\mathbf{V}\tilde{\boldsymbol{x}}, t, \boldsymbol{\gamma}\right) \tag{6}$$

In this way, the original model is transformed into the reduced order model by inserting Eq. (5) and Eq. (6) into Eq. (3).

Different methods are available to determine the weight matrix and the matrix of modes. The method used in this article is proper orthogonal decomposition (POD), where both matrices are the same semi-orthogonal matrix i.e., $\mathbf{V} = \mathbf{W}$ and $\mathbf{V}^{\mathrm{T}}\mathbf{V} = \mathbf{Id}$ (Chatterjee, 2000). It is a method that can be applied to both linear and nonlinear dynamical systems and additionally provides mathematical estimates of errors and sensitivity (Rathinam and Petzold, 2003; Chaturantabut and Sorensen, 2010; Gräßle et al., 2021). Thus, with the POD method it is also possible to investigate more complicated, nonlinear models – a property important for future analyses of the dynamics of core internals.

The matrix of modes $\mathbf{V}$ in POD is determined with a so-called snapshot matrix which is constructed from a transient of the original system $\boldsymbol{x}(t)$. The transient is evaluated at discrete time-steps t_i such that $\boldsymbol{x}_i = \boldsymbol{x}(t_i)$ and $t_{i+1} = t_i + \Delta t$. These snapshots $\boldsymbol{x}_i$ are arranged as columns in the snapshot matrix

$$\mathbf{X} = (\boldsymbol{x}_1 | \cdots | \boldsymbol{x}_N)$$

These snapshots are then approximated by low rank matrices of the form:

$$\mathbf{M} = \sum_{i=1}^{r} \sigma_i \boldsymbol{v}_i \boldsymbol{u}_i^{\mathrm{T}}$$

POD utilizes the optimal approximation of $\mathbf{X}$ in the Frobenius norm by a low rank matrix $\mathbf{O}$, such that $\mathbf{O}$ solves:

$$\min_{\mathrm{rank}(\mathbf{M})=r} \|\mathbf{X} - \mathbf{M}\|_{\mathrm{Fr}} = \mathbf{O}$$

It is a well-known fact that this minimization problem can be solved via a singular value decomposition (SVD) of $\mathbf{X}$:

$$\mathbf{X} = \mathbf{V}\,\Sigma\,\mathbf{U}^{\mathrm{T}} \tag{7}$$

by only considering the first k columns of $\mathbf{U}$ and $\mathbf{V}$ while the dimension of the diagonal matrix Σ is adjusted accordingly (Eckart & Young, 1936). The approximation error of the original transient $\mathbf{X}$ and the approximated version $\hat{\mathbf{X}}$ is given by:

$$\|\mathbf{X} - \hat{\mathbf{X}}\|_{\mathrm{Fr}}^2 = \sum_{i=k+1}^{n} \sigma_i^2$$

5.2. Description of the mechanical reduced order model

The mechanical model used for the full-core investigations is a variant of the mechanical model described in section 3.3. It permits a two-dimensional elongation of the fuel assemblies and is adapted such that it takes all of the fuel assemblies inside the reactor core into account. It also uses four types of fuel assemblies with decreasing lateral stiffness. The fuel assemblies, the core barrel and the reactor pressure vessel are all modelled by linear beams in ANSYS mechanical, as explained in section 3.3. The four different types of fuel assemblies each correspond to different time periods of the fuel assemblies inside the reactor core. The distribution of these fuel assemblies in the simulations is shown in Fig. 16. Since the fuel assemblies are distributed in a two-dimensional pattern inside the core, fluidic-near field forces were not considered in the full-core model, as they would lead to a significant modification of the mechanical model. The investigation presented in the following focusses on a scenario, where the vibration of the fuel assemblies is caused by a vibration of the core barrel and the reactor pressure vessel. The vibrations of these components will trigger

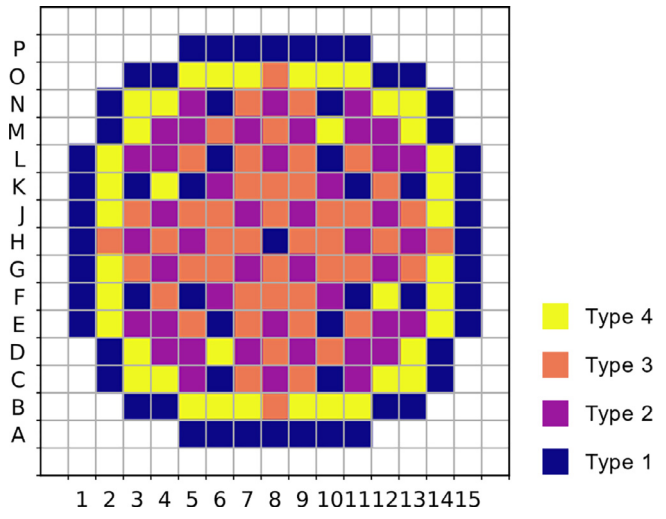

Fig. 16. Distribution of the four types of fuel assemblies in the model. Higher number means lower stiffness.

synchronized vibrations of fuel assemblies with the same mechanical properties through their mechanical coupling between the fuel assemblies and the core barrel/ reactor pressure vessel. This scenario is used to test the coupling and to compare the qualitative agreement of this isolated mechanism to the measurement data. It was chosen, despite the small mechanical coupling found in section 4.2, because it leads to a vibration of all mechanical core components.

ANSYS mechanical uses a finite elements solver for the simulation of the time dependent vibrations of the core components. On this basis, the model can generically be described by a second order differential equation of the following form:

$$\mathbf{M}\,\tfrac{\mathrm{d}^2}{\mathrm{d}t^2}\boldsymbol{x}(t) + \mathbf{D}\,\tfrac{\mathrm{d}}{\mathrm{d}t}\boldsymbol{x}(t) + \mathbf{K}\,\boldsymbol{x}(t) = \boldsymbol{q}(t) \tag{8}$$

where $\boldsymbol{x}$ is the vector of the degrees of freedom (DOFs), $\mathbf{M}$ the mass matrix of the system, $\mathbf{D}$ the damping matrix, $\mathbf{K}$ the stiffness matrix and $\boldsymbol{q}$ represents the external load vector. The damping model used for the simulations is Rayleigh damping i.e., $\mathbf{D} = \alpha\mathbf{M} + \beta\mathbf{K}$. Damping generally reduces the occurrence of peaks in the vibrational signal. Various values were considered for α and β. The investigations showed that the most important parameter to obtain a realistic neutron noise signal with the model is stiffness damping β.

The second order differential equation (8) can be transformed into a first order system, with:

$$\boldsymbol{v}(t) := \tfrac{\mathrm{d}}{\mathrm{d}t}\boldsymbol{x}(t) \tag{9}$$

such that

$$\tfrac{\mathrm{d}}{\mathrm{d}t}\begin{pmatrix}\boldsymbol{x}(t)\\ \boldsymbol{v}(t)\end{pmatrix} = \begin{pmatrix}0 & \mathbf{id}\\ -\mathbf{M}^{-1}\mathbf{K} & -\mathbf{M}^{-1}\mathbf{D}\end{pmatrix}\begin{pmatrix}\boldsymbol{x}(t)\\ \boldsymbol{v}(t)\end{pmatrix} + \begin{pmatrix}0\\ \mathbf{M}^{-1}\end{pmatrix}\boldsymbol{q}(t) \tag{10}$$

The external load vector $\boldsymbol{q}(t)$ of the investigations presented in this section is modeled by a Gaussian white noise random force with zero mean in the x- and y-direction which is applied to the core barrel and the reactor pressure vessel. This represents an idealization of the mechanisms discussed in section 2.3. The standard deviation of the force scales the elongations of the fuel assemblies, which in turn scale the neutron noise signal. Different standard deviations were tested, where a standard deviation of 200 kN was used for all results presented in this article to obtain realistic noise levels for undamped signals. The necessary magnitude of this force confirmed the results from the previous sections and the results in (Viebach et al., 2019). The core barrel/RPV synchronization of the fuel assemblies investigated in the present section is only one effect among many to be considered, which are currently also under investigation (see for example (Viebach et al., 2020) for the effect of synchronized vibrations with rows of fixed fuel assemblies). The investigation is thus a piece towards understanding the whole signal, despite being possibly a smaller contribution if the real forces on the core barrel and RPV are smaller.

This system, Eq. (10), was reduced by POD model order reduction after a sinusoidal perturbation according to the explanation in section 5.2. The dimension $\tilde{n}$ of the reduced order model was chosen such that the relative deviation of the method is given by:

$$\sum_{i=\tilde{n}+1}^{n} \sigma_i^2 \Big/ \sum_{i=1}^{n} \sigma_i^2 \leq 10^{-6}$$

5.3. The DYN3D model and coupling to the mechanical model

The mechanical model is coupled to the system code DYN3D in order to simulate the resulting fluctuations of the neutron flux. The used version of DYN3D (Rohde et al., 2016) solves the time-dependent three-dimensional neutron transport equation consid-

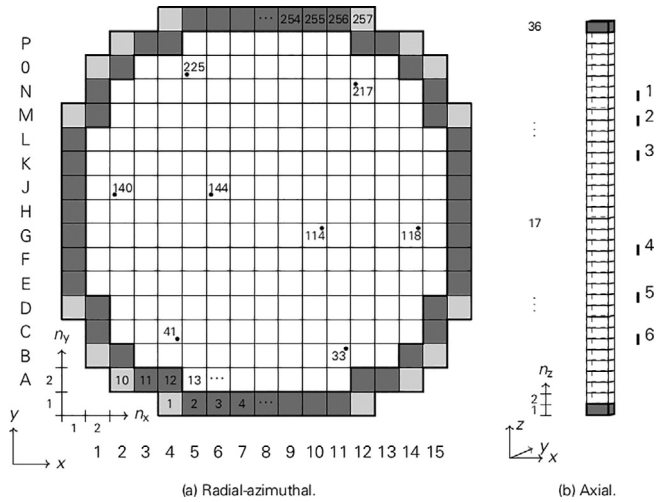

Fig. 17. Nodal setup of the PWR in DYN3D. Detector locations of the in-core detectors are marked with a small dot and with their channel number in DYN3D. The axial position is numbered from 1 to 6 and marked by a bar on the right.

ering two energy groups and using the diffusion approximation for the angular dependency and nodal methods for the spatial dependency. The equations are coupled to the intrinsic one-dimensional thermal-hydraulics module, which represents the coolant flow by four equations for each individual coolant channel, and to the one-dimensional heat-conduction equation for the fuel rods. Fig. 17 presents the nodal setup of the used PWR model, representing a KWU Pre-Konvoi at 100 % power at end of cycle, see (Viebach et al., 2019) for more details.

The simulation of fluctuations of the neutron flux is initialized by a steady-state calculation. In the subsequent time-dependent calculation, the system is externally perturbed by a variation of the fuel-assembly-pitch variable $p_i(z,t), i = 1,2,\cdots,193, t > 0$s, which was added to the DYN3D feedback parameters to incorporate time-dependent fuel-assembly bow, i.e. variations of the fuel-assembly distances $d_{ij}(z,t), j = 1,2,\cdots,8$ in an approximate manner:

$$p_i(z,t) := \frac{1}{4} \cdot \sum_{j_i \in \{1,2,7,8\}} d_{ij_i}(z,t)$$

The fuel assemblies indexed $j_i \in \{1,2\}$ are the x-direction neighbors of the i-th fuel assembly and those indexed $j_i \in \{7,8\}$ are its y-direction neighbors. In order to provide the corresponding branch for the variable $p_i(z,t)$ in the DYN3D cross-section library, which covers the full set of group constants (also assembly discontinuity factors, e.g.), a series of CASMO5 (Studsvik Scandpower Inc.) lattice-code runs were performed under variation of the fuel-assembly pitch p. The time series $p_i(z,t)$ are provided from the mechanical model for each axial layer $z(n_z), n_z = 1,2,\cdots,36$. The values refer to the node centers. And as the axial layers of the mechanical model and the DYN3D model do not match, linear interpolation with respect to the z-direction is used to quantify $p_i(z,t)$ at the DYN3D layers. The time-series are loaded from an external file during the DYN3D run. After the DYN3D simulation, the fluctuations of the nodal power density are evaluated as a measure for the neutron flux fluctuations.

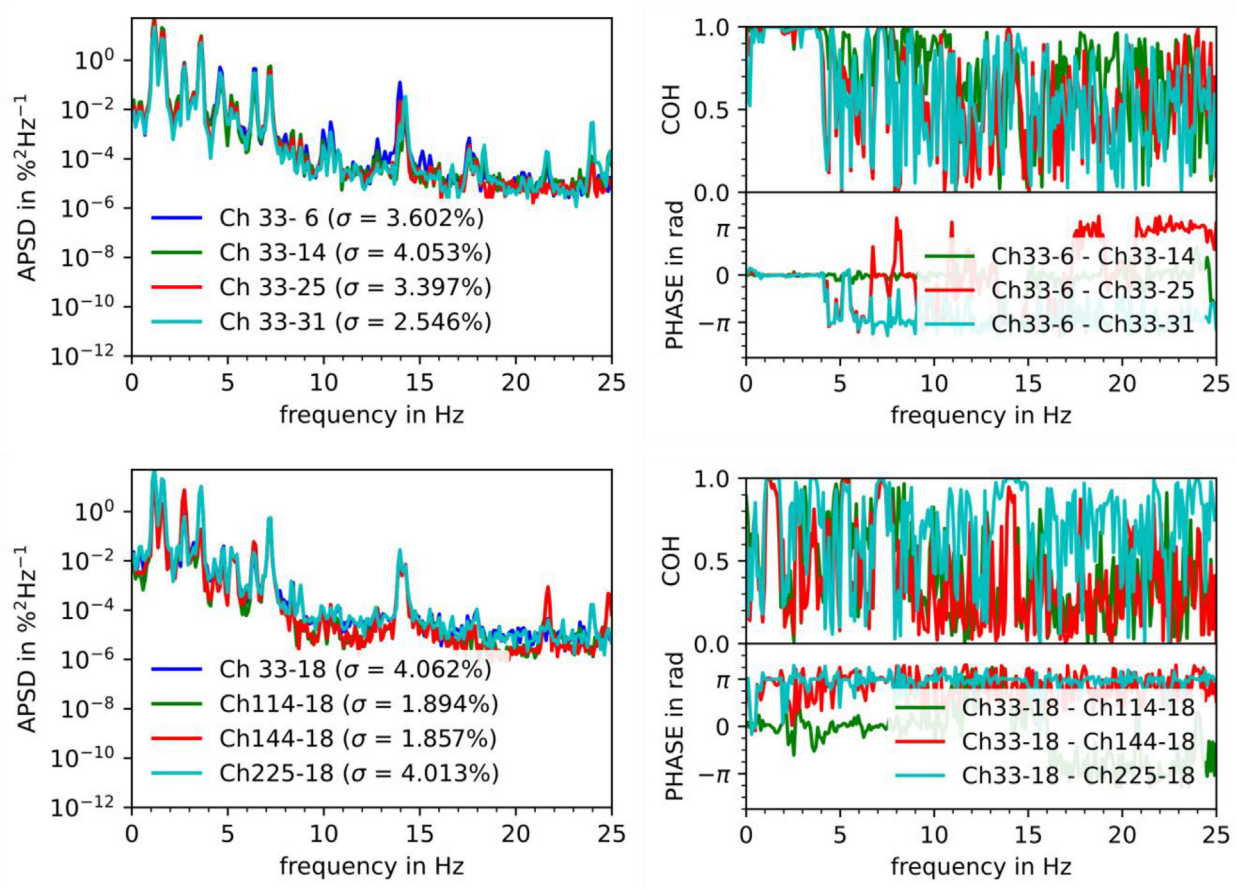

Fig. 18. APSD (left) and coherence and phase (right) of the detector signals with no damping ($\beta = 0$). In the top row is a comparison of the axial layers of a fuel assembly lance and in the bottom row, the azimuthal comparison of different detector positions at mid height.

5.4. Results and discussion

After running the simulations for 40 s, the resulting time-domain signals of the thermal neutron flux at the detector locations in channels 33, 114, 144 and 225 of the DYN3D model were transferred to frequency domain by using Welch's method for cross-power spectral density estimation and the estimation of the coherence and phase of the signals. Four main features of the neutron noise data are used to assess the qualitative agreement with measured data: a maximum in the APSD at around 0.8 Hz, a decrease of the APSD for higher frequencies with $1/f^2$, in phase behavior of axial detectors and in-phase behavior of in-core neutron detectors in the same core half and out-of-phase behavior of in-core neutron detectors in the opposite core half, see for example (Seidl et al., 2015; Viebach, 2019).

The stiffness coefficients α and β were varied between 0 and 0.1. Two exemplary cases of this variation of the damping coefficient β with zero mass damping coefficient α are shown in Fig. 18 and Fig. 19. As expected, the APSDs of the signals show distinctive peaks for small stiffness damping coefficient β, which vanish if β is increased. With a stiffness damping coefficient of 0.05, the APSD shows the typical peak at around 1 Hz and a decrease for higher frequencies although steeper than $1/f^2$.

For higher damping coefficient β, the axial coherence is near one with all signals being in phase. An interesting aspect of the results is that the undamped signal shows a phase shift of $-\pi$ in the range from 4 -7 Hz between the lower half and the higher half of the axial signal. A similar behavior can also be seen in measurement data, see e.g. (Viebach et al., 2019). This characteristic is retained for small values of β, but vanishes for higher damping values.

The radial graphs show the characteristic phase shift of $\pm\pi$ for detectors in the opposite core halves, but the coherence is too high for high frequencies, which is attributed to the artificial scenario of neglecting local perturbations of the fuel assemblies and no near field coupling. Also, the detector in channel 144 (L-J06) is in-phase for frequencies between 2 and 6 Hz.

Overall, the damped signals have smaller standard deviation which is because of the fact that more energy is dissipated due to the damping. The forces necessary to generate a realistic amplitude with only a stimulation of the core barrel and the RPV needed to be about 100 times larger than simulated and therefore unrealistically large. It is expected that the synchronization of fuel assembly vibrations by the core barrel and the RPV is only one component of the overall features of the detector noise signal. Nevertheless, the study showed that under the simple assumptions: insignificant interaction between the fuel assemblies, no local perturbation of the fuel assemblies and a stochastic force acting on the core barrel and reactor pressure vessel, some important characteristics of the neutron noise signal could be reproduced. Additionally, the investigations showed that it was possible to couple a reduced order model of a more realistic mechanical model to a diffusion code to obtain qualitatively accurate noise signals. Therefore, the authors are affirmed in believing a model of the mechanical vibrations inside the core must be considered in the search for the understanding of the neutron noise signal in light water power reactors.

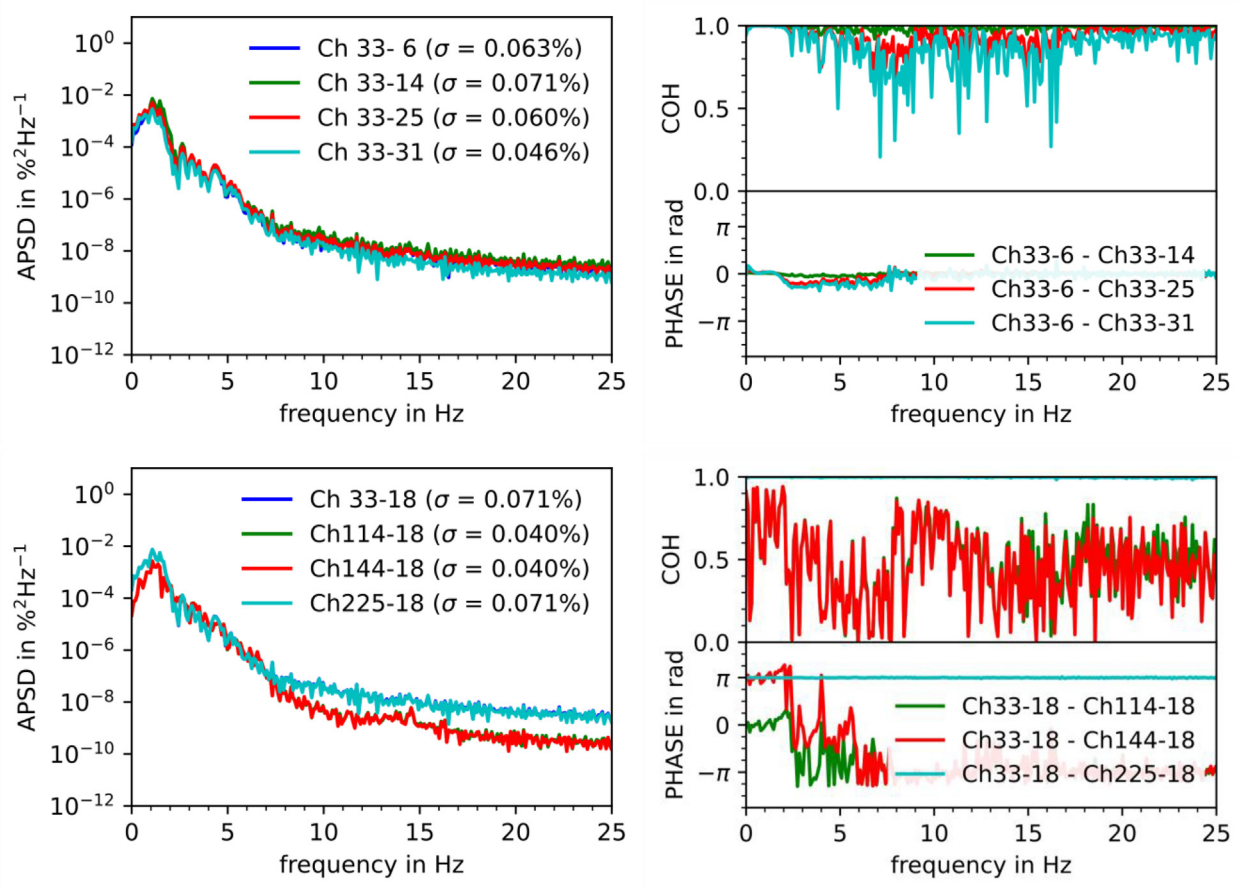

Fig. 19. APSD (left) and coherence and phase (right) of the detector signals at a stiffness damping coefficient $\boldsymbol{\beta} = 0.05$. In the top row is a comparison of the axial layers of a fuel assembly lance and in the bottom row, the azimuthal comparison of different detector positions at mid height.

6. Conclusion and outlook

The paper first describes a comprehensive compilation of mechanical components with an effect on neutron flux while vibrating. Further, a simple mechanical model is developed, which describes the dynamic motion response of the system of RPV, core barrel and a row of fuel assemblies and takes reactive fluidic forces into account. The dynamic answers of the model to different generic excitation scenarios and parametric studies reveal some distinct properties of the system. Overall, the findings affirm the hypothesis that core-wide oscillations of the fluid flow leading to a simultaneous oscillation of individual fuel assembly groups, in combination with changes of fuel assemblies' mechanical properties, might be responsible for the temporary increase of neutron flux fluctuations observed in some PWR built by KWU. A variant of the model was coupled to the reactor dynamics code DYN3D in order to simulate neutron noise. The model reproduces important features of the observed signals, while being overall too low in noise amplitude. It shows the possibility of the usage of model order reduction techniques for future coupled full core FSI simulations to reduce the computation time.

The described approach of using a simple mechanical model with the fluidic reaction described as added mass, stiffness and damping is capable of qualitatively describing important aspects of the dynamic behavior of the RPV internals while being simple, robust and efficient in terms of computational costs. Future improvements could encompass the investigation of the effect of collisions among the fuel assemblies and the core shroud, the inclusion of further components with effect on neutron flux measurement and the application of further generic excitation scenarios. Nevertheless, the approach may eventually reach its limits and, to simulate a broader spectrum of effects and a more realistic component and fluid behavior, a fully included bidirectional FSI model with a detailed numerical consideration of the fluid becomes necessary. The simple model gives some clues for the more detailed model, e.g. that the RPV/core barrel could be considered separately from a mechanical point of view. Fully included bidirectional FSI models have already been generated for seismic analysis, e.g. in (Broc et al., 2003) or (Ricciardi, 2016). Alternatively, advanced models for the investigation of static fuel assembly deformation, like in (Marx & Wicklein, 2012) or (Lascar et al., 2015) could be enhanced for dynamic simulations.

In addition to simulation efforts, on-site evaluation of neutron-flux sensors, pressure gauges, displacement transducers, thermocouples, accelerometers or main coolant pump supply current under normal and special flow conditions (commissioning tests, start-up/shutdown, partial load, 3/4 main coolant pumps) and correlation among these sensor signals could reveal further insights into the phenomena and help to develop models. The integration of additional measurement systems into the core for fuel assembly and core barrel vibration and flow field velocity measurement may be difficult when done in the running reactor instead of in a mock-up or before commissioning, although such projects have been successfully done in the past (Laggiard et al., 1995). Furthermore, such measurements would allow only a punctual quantification without necessarily discovering the complete nature of the phenomenon. Interdisciplinary work between utilities, experimentalists and simulation experts of all involved disciplines is therefore a key aspect in further research.

Declaration of Competing Interest

The authors declare that they have no known competing financial interests or personal relationships that could have appeared to influence the work reported in this paper.

Acknowledgements

The CORTEX research project has received funding from the Euratom research and training programme 2014-2018 under grant agreement No 754316.

References

ANSYS Inc., 2019. ANSYS 2019R1. Canonsburg, PA, USA.
Altstadt, E., Grunwald, G., Scheffler, M., Weiß, F.-P., 1997. Analytische Modellierung mechanischer Schwingungen von Primärkreiskomponenten des Druck wasserreaktors WWER-440 mit finiten Elementen. Forschungszentrum Rossendorf, FZR-172 https://nbn-resolving.org/urn:nbn:de:bsz:d120-qucosa-31243.
Altstadt, E., Weiß, F.-P., 1999. Finite Element based vibration analysis of WWER-440 type reactors. Annals of Nuclear Energy 26 (12), 1037–1052. https://doi.org/10.1016/S0306-4549(99)00002-X.
Antoulas, A.C., Sorensen, D.C., Gugercin, S., 2001. A survey of model reduction methods for large-scale systems. American Mathematical Society 280, 193–219. https://doi.org/10.1090/conm/280.
Areva Inc., 2010. HTP: Robust Technology for PWR Fuel Assemblies. Brochure.
Au-Yang, M.K., Brenneman, B., Raj, D., 1995. Flow-induced vibration test of an advanced water reactor model Part 1: turbulence-induced forcing function. Nuclear Engineering and Design 157, 93–109. https://doi.org/10.1016/0029-5493(95)00980-Q.
Axisa, F., 1993. A Decade of Progress in Flow-Induced Vibration. Stuttgart, Germany, SMiRT-12, https://www.lib.ncsu.edu/resolver/1840.20/23894.
Bauernfeind, V., 1977. Investigations on the vibrative excitation of PWR pressure vessel and internals by pressure noise analysis and model calculations. Progress in Nuclear Energy 1 (2–4), 323–332. https://doi.org/10.1016/0149-1970(77)90088-9.
Bauernfeind, V., 1988. Vibration monitoring of a four-loop PWR: Model-investigations of the sensitivity of the monitored signals on mechanical failures. Progress in Nuclear Energy 21, 247–254. https://doi.org/10.1016/0149-1970(88)90041-8.
Baur, U., Benner, P., Feng, L., 2014. Model order reduction for linear and nonlinear systems: a system-theoretic perspective. Max Planck Institute Magdeburg Preprints 21 (4), 331–358.
Banyay, G.A., Imbrogno, G.M., Meyer, G.A., 2013. Generation of Pump-Induced Pulsation Loads For the AP1000 Reactor Internals. San Francisco, CA, USA, SMiRT-22, https://www.lib.ncsu.edu/resolver/1840.20/32882.
Billerey, A., 2005. Evolution of Fuel Rod Support under Irradiation - Impact on the Mechanical Behaviour of Fuel Assemblies. Proceedings of a technical meeting held in Cadarache, France, IAEA-TECDOC-1454. https://www.iaea.org/publications/7286/structural-behaviour-of-fuel-assemblies-for-water-cooled-reactors.
Blevins, R.D., 1979. Flow-induced vibration in nuclear reactors: A review. Progress in Nuclear Energy 4 (1), 25–49. https://doi.org/10.1016/0149-1970(79)90008-8.
Borsoi, L., 2001. Flow-Induced Vibration of Nuclear Components - Future R&D Perspective Derived from the French Experience. Washington, DC, USA, SMiRT-16, https://www.lib.ncsu.edu/resolver/1840.20/30712.
Broc, D., Queval, J.-C., Viallet, E., 2003. Seismic Behaviour of a PWR Reactor Core: Fluid Structure Interaction Effects. Prague, Czech Republic. Czech Republic SMiRT-17 https://www.lib.ncsu.edu/resolver/1840.20/27350.
Chatterjee, A., 2000. An introduction to the proper orthogonal decomposition. Current Science 78 (7), 808–817. https://www.jstor.org/stable/24103957.
Chaturantabut, S., Sorensen, D.C., 2010. Nonlinear model reduction via discrete empirical interpolation. SIAM Journal on Scientific Computing 32 (5), 2737–2764. https://doi.org/10.1137/090766498.
Chen, S.S., 1983. Flow Induced Vibration and Instability of Some Nuclear Reactor System Components. Chicago, IL, USA, SMiRT-7, http://www.lib.ncsu.edu/resolver/1840.20/25784.
Collard, B., 2004. Flow Induced Damping of a PWR Fuel Assembly. Proceedings of a technical meeting held in Cadarache, France, IAEA-TECDOC-1454. https://www.iaea.org/publications/7286/structural-behaviour-of-fuel-assemblies-for-water-cooled-reactors.
Conner, M.E., Smith, L.D., Paramonov, D.V., Liu, B., Dzodzo, M., 2003. 2003. Understanding and predicting the flow field in a reactor core, Würzburg, Germany, TopFuel.
Dach, K. et al., 1985. The experiences of using neutron noise analysis for vibration behaviour of internal structures. Progress in Nuclear Energy 15, 243–250. https://doi.org/10.1016/0149-1970(85)90047-2.
Damiano, B., Kryter, R.C., 1990. Current Applications of Vibration Monitoring and Neutron Noise Analysis. Oak Ridge National Laboratory, NUREG/CR-5479.
Demazière, C., 2017. Neutron noise-based core monitoring for identifying and characterizing anomalities and their root causes in operating reactors. Berlin, Germany, 48th Annual Meeting on Nuclear Technology.
Demazière, C. et al., 2018. Overview of the CORTEX project. Cancun, Mexico, PHYSOR 2018. https://doi.org/10.5281/zenodo.1244166.
Eckart, C., Young, G., 1936. The approximation of one matrix by another of lower rank. Psychometrika 1 (3), 211–218. https://doi.org/10.1007/BF02288367.
Fiedler, J., 2002. Schwingungsüberwachung von Primärkreiskomponenten in Kernkraftwerken. University of Hannover. Dissertation.

Fontaine, B., Politopoulos, I., 2000. A non linear model for the PWR fuel assembly seismic analysis. Nuclear Engineering and Design 195 (3), 321–329. https://doi.org/10.1016/S0029-5493(99)00217-4.
Fry, D.N., Kryter, R.C., Robinson, J.C., 1974. Analysis of Neutron Density Oscillations Resulting from Core Barrel Motion in the Palisades Nuclear Power Plant. Oak Ridge National Laboratory, ORNL-TM-4570.
Fry, D.N., March-Leube, J., Sweeney, F.J., 1984. Use of Neutron Noise for Diagnosis Of In-Vessel Anomalies in Light-Water Reactors. Union Carbide Corporation, NUREG/CR-3303.
Fujita, K., 1990. Flow-induced vibration and fluid-structure interaction in nuclear power plant components. Journal of Wind Engineering and Industrial Aerodynamics 33 (1–2), 405–418. https://doi.org/10.1016/0167-6105(90)90056-I.
Gräßle, C., Hinze, M., Volkwein, S., 2021. Model order reduction by proper orthogonal decomposition, Model Order Reduction: Volume 2: Snapshot-Based Methods and Algorithms. De Gruyter.
Grondey, G., Harms, R., Kumpf, H., Winderl, G., 1991. Low frequency noise in a PWR and its influence on the normal operational characteristics of the plant. Proceedings of a Specialists' Meeting held in Pittsburg, CA, USA.
Grunwald, G., Hessel, G., Liewers, P., Schmitt, W., 1982. Low frequency pressure oscillations in a PWR. Progress in Nuclear Energy 9, 569–579. https://doi.org/10.1016/0149-1970(82)90076-2.
Haslinger, K.H., Joffre, P.F., Nordström, L., Andersson, S., 2001. Flow Induced Vibration Testing of a PWR Fuel Assembly. Washington, DC, USA, SMiRT-16, https://www.lib.ncsu.edu/resolver/1840.20/30515.
Herb, J., Bläsius, C., Küntzel, M., 2016. Untersuchungen der Ursachen für Neutronenflussschwankungen. GRS gGmbH, GRS - 408, ISBN 978-3-944161-90-7.
Herb, J., Bläsius, C., Perin, Y., Sievers, J., Velkov, K., 2018. Analyses of Possible Explanations for the Neutron Flux Fluctuations in German PWR. atw 62 (8/9), 446–451.
Hollstein, F., 1995. Berechnung von Neutronenflußdichteschwankungen in WWER-Druckwasserreaktoren infolge strömungsinduzierter Schwingungen. Forschungszentrum Rossendorf, FZR-110. https://nbn-resolving.org/urn:nbn:de:bsz:d120-qucosa-31769.
Horváth, Á., Dressel, B., 2013. On numerical simulations of fuel assembly bow in pressurized water reactors. Nuclear Engineering and Design 265, 814–825. https://doi.org/10.1016/j.nucengdes.2013.09.031.
Jeon, S.Y. et al., 2009. An Investigation on the Fuel Assembly Structural Performance for the PLUS7 Fuel Design. Espoo, Finland, SMiRT-20, http://www.lib.ncsu.edu/resolver/1840.20/23814.
Kaneko, S. et al., 2014. Flow-Induced Vibrations - Classifications and Lessons from Practical Experiences. 2nd Edition Elsevier.
Laggiard, E. et al., 1995. Vibration measurements in PWR obrigheim by use of in-core accelerometers. Progress in Nuclear Energy 29 (3–4), 229–238. https://doi.org/10.1016/0149-1970(95)00010-H.
Lascar, C. et al., 2015. Advanced Predictive Tool for Fuel Assembly Bow based on 3D Coupled FSI Approach. Zurich, Switzerland, TopFuel.
Liewers, P., Schmitt, W., Schumann, P., Weiß, F.-P., 1988. Detection of core barrel motion at WWER-440-type reactors. Progress in Nuclear Energy 21, 89–96. https://doi.org/10.1016/0149-1970(88)90023-6.
Lu, R.Y., Seel, D.D., 2006. PWR Fuel Assembly Damping Characteristics ICONE-14.
Marx, V., Wicklein, M., 2012. Status of fuel assembly bow modeling. Stuttgart, Germany, 43th Annual meeting on nuclear technology.
Mitzel, F., Väth, W., Ansari, S., 1982. Nachweis von Brennelementschwingungen in KNK II. Kernforschungszentrum Karlsruhe, KfK 3379.
Morales, M., Cerracin, A., Aleshin, Y., Kim, J.H., 2012. SAVAN3D: Improving simulation capabilities of SAVAN technology. Manchester, UK, TopFuel.
Mulcahy, T.M., 1983. A review of leakage-flow-induced vibrations of reactor components. Argonne National Laboratory, ANL–83-43.
O'Cain, M.B., 2013. Root Cause Analysis Summary - Krsko Cycle 26 Leaking Fuel Assemblies. Westinghouse, CAPS 13–282-C025, PE-14-8.
Païdoussis, M.P., 2016. Fluid-Structure Interactions - Slender Structures and Axial Flow. Elsevier, ISBN 978-0-12-397333-7.
Païdoussis, M.P., 1982. A review of flow-induced vibrations in reactors and reactor components. Nuclear Engineering and Design 74 (1), 31–60. https://doi.org/10.1016/0029-5493(83)90138-3.
Païdoussis, M.P., 2006. Real-life experiences with flow-induced vibration. Journal of Fluids and Structures 22 (6–7), 741–755. https://doi.org/10.1016/j.jfluidstructs.2006.04.002.
Palamera, M.J. et al., 2015. Development of an advanced PWR reactor Internals System Finite Element Model for Flow-Induced Vibration Analysis. Boston, MA, USA, ASME PVP 2015. https://doi.org/10.1115/PVP2015-45278.
Paramonov, D.V., Young, M.Y., Jiang, J.X., 2001. The Flow Field in a Reactor Core and its Effect on Rod Vibration and Wear. Proceedings of a Symposium on Flow-Induced Vibration, Atlanta, GA, USA, ASME PVP 2001.
Pettigrew, M.J. et al., 1998. Flow-induced vibration: recent findings and open questions. Nuclear Engineering and Design 185 (2–3), 249–276. https://doi.org/10.1016/S0029-5493(98)00238-6.
Pisapia, S., Collard, B., Bellizi, S., Mori, V., 2003. Modal Testing and Identification of a PWR Fuel Assembly. Prague, Czech Republic, SMiRT-17, https://www.lib.ncsu.edu/resolver/1840.20/27052.
Pohlus, J., Paquée, U., 2018. Untersuchung veränderter Neutronen flussschwankungen und Brennstab-Beanspruchungen in DWR-Anlagen im Rahmen der Sicherheitsforschung. TÜV Rheinland ISTec GmbH, ISTec - A - 3695.
Rathinam, M., Petzold, L.R., 2003. A new look at proper orthogonal decomposition. SIAM Journal on Numerical Analysis 41 (5), 1893–1925. https://doi.org/10.1137/S0036142901389049.
Ricciardi, G., Bellizzi, S., Collard, B., Cochelin, B., 2009a. Modelling Pressurized Water Reactor cores in terms of porous media. Journal of Fluids and Structures 25 (1), 112–133. https://doi.org/10.1016/j.jfluidstructs.2008.04.002.
Ricciardi, G., Bellizzi, S., Collard, B., Cochelin, B., 2009b. Row of fuel assemblies analysis under seismic loading: Modelling and experimental validation. Nuclear Engineering and Design 239 (12), 2692–2704. https://doi.org/10.1016/j.nucengdes.2009.08.029.
Ricciardi, G., 2016. Fluid-structure interaction modelling of a PWR fuel assembly subjected to axial flow. Journal of Fluids and Structures 62, 156–171. https://doi.org/10.1016/j.jfluidstructs.2016.01.006.
Ricciardi, G., 2017. Dynamical Nonlinear Modelling of a Pressurised Water Reactor Fuel Assembly Subjected to an Axial Flow. Rome, Italy, 10th EURODYN.
Ricciardi, G., Boccaccio, E., 2015. Modelling of the flow induced stiffness of a PWR fuel assembly. Nuclear Engineering and Design 282, 8–14. https://doi.org/10.1016/j.nucengdes.2014.11.027.
Rigaudeau, J., Brochard, D., Benjedidia, A., 1993. Fluid Structure Interaction in the Response of PWR Fuel Assemblies to Horizontal Seismic Loads. Stuttgart, Germany, SMiRT-12, https://www.lib.ncsu.edu/resolver/1840.20/24403.
Rohde, U. et al., 2016. The reactor dynamics code DYN3D - models, validation and applications. Progress in Nuclear Energy 89, 170–190. https://doi.org/10.1016/j.pnucene.2016.02.013.
Runkel, J., 1987. Rauschanalyse in Druckwasserreaktoren. University of Hannover. Dissertation.
Runkel, J. et al., 1997. In-Core Measurements of Reactors Internals Vibrations by Use of Accelerometers and Neutron Detectors. Proceedings of a Specialist meeting in Mito-shi, Japan.
Schumann, P., 2000. Nutzung der Rauschdiagnostik für Nachweis und Überwachung der Schwingungen von Reaktordruckbehältereinbauten und zur Aufklärung ihrer Ursachen in ostdeutschen Kernkraftwerken mit WWER-440/230-Reaktoren der russischen Baureihe. Forschungszentrum Rossendorf, FZR-304.
Seidl, M., Kosowski, K., Schüler, U., Belblidia, L., 2015. Review of the historic neutron noise behavior in German KWU built PWRs. Progress in Nuclear Energy 85, 668–675. https://doi.org/10.1016/j.pnucene.2015.08.016.
Shah, S.J., Brenneman, B., Rigadeau, J., 2001. Comparison of Analytical and Experimental Damping Under Axial Flow for Different Fuel Assembly Types. Nice. Italy ICONE-9.
Snyder, M. et al., 2003. AP1000 Reactor Internals Flow-Induced Vibration Assessment Program. AP1000 Document APP-MIO1-GER-001, Revision 1.
Stegemann, D., Runkel, J., 1995. Experience with Vibration Monitoring in German PWRs Obrigheim, Grohnde, Brokdorf and Emsland. SMORN-VII, Paris, France.
Stabel, J., Ren, M. Ladouceur, B., 2005. New Knowledge and Experiences of Flow Induced Fretting in PWR Fuel Assemblies. Beijing, PRC, SMiRT-18, https://www.lib.ncsu.edu/resolver/1840.20/31448.
Studsvik Scandpower Inc., CASMO5. A Fuel Assembly Burnup Program.
Stulík, P., Torres, L., Montalvo, C., García-Berrocal, A., 2019. Development of advanced signal processing techniques and evaluation results, Deliverable 3.3 of the EU CORTEX project.
Sunder, R., 1985. Sammlung von Signalmustern zur DWR Schwingungsüberwachung - Informationsgehalt der Neutronenfluss rauschsignale. GRS gGmbH, GRS - A - 1074.
Thie, J.A., 1981. Power Reactor Noise. American Nuclear Society.
Trenty, A., 1995. Operational Feedback on Internal Structure Vibration in 54 French PWRs during 300 Fuel Cycles. Progress in Nuclear Energy 29 (3–4), 347–356. https://doi.org/10.1016/0149-1970(95)00017-E.
Viallet, E., Kestens, T., 2003. Prediction of Flow Induced Damping of a PWR Fuel Assembly in Case of Seismic and Loca Load Case. Prague. Czech Republic SMiRT-17 https://www.lib.ncsu.edu/resolver/1840.20/27049.
Viebach, M. et al., 2019. Simulation of low-frequency PWR neutron flux fluctuations. Progress in Nuclear Energy 117, 103039. https://doi.org/10.1016/j.pnucene.2019.103039.
Viebach, M. et al., 2020. Neutron Noise Patterns from Coupled Fuel-Assembly Vibrations, Cambridge, UK, PHYSOR.
Viebach, M. et al., 2022. Verification of the code DYN3D for calculations of neutron flux fluctuations. Annals of Nuclear Energy 166, 108735. https://doi.org/10.1016/j.anucene.2021.108735.
Wach, D., Sunder, R., 1977. Improved PWR-neutron noise interpretation based on detailed vibration analysis. Progress in Nuclear Energy 1 (2–4), 309–322. https://doi.org/10.1016/0149-1970(77)90087-7.
Wach, D. & Sunder, R., 1989. Long-Term Vibration Trending as a Basis for Performance Assessment and Life Extension of Mechanical Components, Anaheim, CA, USA, SMiRT-10, http://www.lib.ncsu.edu/resolver/1840.20/29279.
Wanninger, A., Seidl, M., Macián-Juan, R., 2016a. Development of computational methods to describe the mechanical behavior of PWR fuel assemblies, Hamburg, Germany, 47th Annual Meeting on Nuclear Technology.
Wanninger, A., Seidl, M. Macián-Juan, R., (2016b) Screening sensitivity analysis of a PWR fuel assembly FEM structural model. Boise, ID, USA, Top Fuel 2016.
Wanninger, A., 2018. Mechanical Analysis of the Bow Deformation of Fuel Assemblies in a Pressurized Water Reactor Core. Technical University of Munich, Dissertation.
Wehling, H.J., Klinger, K., Stölben, H., 1985. The influence of thermohydraulic parameters on the dynamic behaviour of KWU-PWR's. Progress in Nuclear Energy 15, 273–282. https://doi.org/10.1016/0149-1970(85)90050-2.

Wei, Z., 2015. Predictive Study of CAP1400 Core Barrel Flow-induced Vibration Part 1: Turbulence induced Forcing Function. Manchester, UK, SMiRT-23, http://www.lib.ncsu.edu/resolver/1840.20/34105.

Witters, F., 2004. Fluid Damping on Fuel Assemblies under Axial Flow. Proceedings of a technical meeting held in Cadarache, France, IAEA-TECDOC-1454. https://www.iaea.org/publications/7286/structural-behaviour-of-fuel-assemblies-for-water-cooled-reactors.

Yun Je, S., Chang, Y.S., Kang, S.S., 2017. Dynamic characteristics assessment of reactor vessel internals with fluid-structure interaction. Nuclear Engineering and Technology 49 (7), 1513–1523. https://doi.org/10.1016/j.net.2017.05.003.

Zeman, V., Hlaváč, Z., 2008. Dynamic Response of VVER 1000 Type Reactor Excited by Pressure Pulsations. Engineering Mechanics 15 (6), 435–446.